

Cal-QL: Calibrated Offline RL Pre-Training for Efficient Online Fine-Tuning

Mitsuhiko Nakamoto^{1*}, Yuexiang Zhai^{1*}, Anikait Singh¹, Max Sobol Mark², Yi Ma¹, Chelsea Finn², Aviral Kumar¹ and Sergey Levine¹

*Equal contributions, ¹UC Berkeley, ²Stanford University

Abstract: A compelling use case of offline reinforcement learning (RL) is to obtain a policy initialization from existing datasets, which allows efficient fine-tuning with limited amounts of active online interaction. However, several existing offline RL methods tend to exhibit poor online fine-tuning performance. On the other hand, online RL methods can learn effectively through online interaction, but struggle to incorporate offline data, which can make them very slow in settings where exploration is challenging or pre-training is necessary. In this paper, we devise an approach for learning an effective initialization from offline data that also enables fast online fine-tuning capabilities. Our approach, calibrated Q-learning (Cal-QL) accomplishes this by learning a conservative value function initialization that underestimates the value of the learned policy from offline data, while also being calibrated, in the sense that the learned Q-values are at a reasonable scale. We refer to this property as calibration, and define it formally as providing a lower bound on the true value function of the learned policy and an upper bound on the value of some other (suboptimal) reference policy, which may simply be the behavior policy. We show that offline RL algorithms that learn such calibrated value functions lead to effective online fine-tuning, enabling us to take the benefits of offline initializations in online fine-tuning. In practice, Cal-QL can be implemented on top of existing conservative methods for offline RL within a one-line code change. Empirically, Cal-QL outperforms state-of-the-art methods on **10/11** fine-tuning benchmark tasks that we study in this paper.

1. Introduction

Modern machine learning successes across many domains follow a common recipe: first pre-training large and expressive models on general-purpose, Internet-scale data, followed by fine-tuning the pre-trained initialization on a limited amount of data for the task of interest (He et al., 2022; Devlin et al., 2018). How can we translate such a recipe to sequential decision-making problems? A natural way to instantiate this paradigm is to utilize offline reinforcement learning (RL) algorithms (Levine et al., 2020) for initializing value functions and policies from previously collected static datasets, followed by task-specific online fine-tuning that aims to improve this initialization with the smallest amount of active interaction. If successful, such a recipe might enable effective and generalizable online RL with significantly fewer samples than current RL methods that learn from scratch.

Many algorithms for offline RL have been applied to online fine-tuning. Empirical results across prior works suggest a counter-intuitive trend: policy initializations obtained from more effective offline RL methods tend to exhibit worse online fine-tuning performance, even within the same task (see Table 2 of Kostrikov et al. (2021b) & Figure 4 of Xiao et al. (2023)). On the other end, online RL methods training from scratch (or RL from demonstrations (Vecerik et al., 2017), where the replay buffer is seeded with the offline data) seem to improve online at a significantly faster rate. But these online methods require actively collecting data by rolling out policies from scratch, which inherits similar limitations of naïve online RL methods in problems where data collection is expensive or dangerous. Overall, these results suggest that it is challenging to devise an offline RL algorithm that both acquires a good initialization from prior data and also enables efficient fine-tuning.

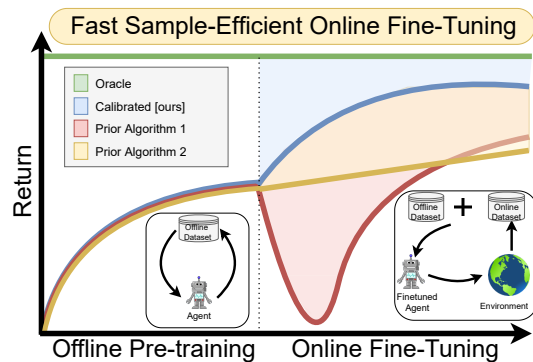


Figure 1: We study the problem of **offline RL pre-training followed by online RL fine-tuning**. Some prior offline RL methods tend to exhibit slow performance improvement in this setting (yellow), resulting in worse asymptotic performance. Others suffer from initial performance degradation once online fine-tuning begins (red), resulting in a high cumulative regret. We develop an approach that “calibrates” the learned value function to attain a fast improvement with a smaller regret (blue).

How can we devise a method to learn an effective policy initialization that also improves during fine-tuning? Prior work (Kumar et al., 2020; Cheng et al., 2022) shows that one can learn a good policy initialization by optimizing the policy against a *conservative* value function obtained from an offline dataset. But, as we show in Section 4.1, conservatism alone is insufficient for efficient online fine-tuning. Conservative methods often tend to “unlearn” the policy initialization learned from offline data and waste samples collected via online interaction in recovering this initialization. We find that this sort of a “unlearning” phenomenon is a consequence of the fact that value estimates produced via conservative methods can be significantly lower than the ground-truth return of *any* valid policy. Having Q-value estimates that do not lie on a similar scale as the return of a valid policy is problematic: once fine-tuning begins, actions executed in the environment for exploration that are actually worse than the policy learned from offline data could erroneously appear better, if their ground-truth return value is larger than the learned conservative value estimate. Hence, subsequent policy improvement will begin to lose the initialization in favor of such a worse policy until the method recovers.

If we can ensure that the conservative value estimates learned using the offline data are *calibrated*, meaning that these estimates are on similar scales as the true return values, then we can avoid the unlearning phenomenon caused by conservative methods. Of course, we cannot enforce such a condition perfectly, since it would require eliminating all errors in the value function. Instead, we devise a method for ensuring that the learned values upper bound the true value of some *reference policies* whose values can be estimated more easily, (e.g., the behavior policy) while still lower bounding the value of the learned policy. Though this does not perfectly ensure that the learned values are correct, we show that it still leads to sample-efficient online fine-tuning. Thus, our practical method, **calibrated Q-learning (Cal-QL)**, learns conservative value functions that are “calibrated” against the behavior policy, via a simple modification to existing conservative offline RL methods.

The main contribution of this paper is Cal-QL, a method for acquiring an offline initialization that facilitates online fine-tuning. Cal-QL aims to learn conservative value functions that are calibrated with respect to a reference policy (e.g., the behavior policy). Our analysis of Cal-QL shows that Cal-QL attains stronger guarantees on cumulative regret during fine-tuning. In practice, Cal-QL can be implemented on top of conservative Q-learning (Kumar et al., 2020), a prior offline RL method, without any additional hyperparameters. We evaluate Cal-QL across a range of benchmark tasks from Fu et al. (2020), Singh et al. (2020) and Nair et al. (2020a), including robotic manipulation and navigation. We show that Cal-QL matches or outperforms the best methods on all tasks, in some cases by 30-40%.

2. Related Work

Several prior works suggest that online RL methods typically require a large number of samples (Silver et al., 2016; Vinyals et al., 2019; Ye et al., 2020; Kakade and Langford, 2002; Zhai et al., 2022; Gupta et al., 2022; Li et al., 2022) to learn from scratch. We can utilize offline data to accelerate online off-policy RL algorithms. Prior works instantiate this idea in a variety of ways: incorporating the offline data into the replay buffer of online RL (Schaal, 1996; Vecerik et al., 2017; Hester et al., 2018; Song et al., 2023), utilizing auxiliary behavioral cloning losses with policy-gradients (Rajeswaran et al., 2017; Kang et al., 2018; Zhu et al., 2018; 2019), or extracting a high-level skill space for downstream online RL (Gupta et al., 2019; Ajay et al., 2020). While these methods improve the sample efficiency of online RL from scratch, as we will also show in our results, they do not eliminate the need to actively roll out poor policies for data collection.

To address this issue, a different line of work aims to first run offline RL for learning a good policy and value initialization from the offline data, followed by online fine-tuning (Nair et al., 2020b; Kostrikov et al., 2021a; Lyu et al., 2022; Beeson and Montana, 2022; Wu et al., 2022; Lee et al., 2022; Mark et al., 2022). These approaches typically employ existing offline RL methods based on policy constraints or pessimism (Fujimoto et al., 2018a; Siegel et al., 2020; Guo et al., 2020; Ghasemipour et al., 2021; Kostrikov et al., 2021a; Singh et al., 2020; Lee et al., 2022) on the offline data for some training epochs, then continue training with the same method on a combination of offline and online data once fine-tuning begins (Nachum et al., 2019; Kidambi et al., 2020; Yu et al., 2020; Kumar et al., 2020; Buckman et al., 2020). Although pessimism is crucial for offline RL (Jin et al., 2021b; Cheng et al., 2022), using pessimism or constraints for fine-tuning (Nair et al., 2020b; Kostrikov et al., 2021a; Lyu et al., 2022) slows down fine-tuning or leads to initial unlearning, as we will show in Section 4.1. In effect, these prior methods either fail to improve as fast as online RL or lose the initialization from offline RL. We aim to address this limitation by understanding some conditions on the offline initialization that enable fast fine-tuning and then turn these conditions into a fine-tuning method – Cal-QL.

Our work is most related to methods that utilize a pessimistic RL algorithm for offline training but incorporate exploration bonuses in fine-tuning (Lee et al., 2022; Mark et al., 2022; Wu et al., 2022). In contrast to these works, our method aims to learn a better offline initialization that enables standard online fine-tuning. Our approach fine-tunes naively without ensembles (Lee et al., 2022) or exploration bonuses (Mark et al., 2022) and, as we show in our experiments, this alone is enough to outperform approaches that utilize exploration bonuses.

3. Preliminaries and Background

The goal in RL is to learn the optimal policy for an MDP $\mathcal{M} = (\mathcal{S}, \mathcal{A}, P, r, \rho, \gamma)$. \mathcal{S}, \mathcal{A} denote the state and action spaces. $P(s'|s, a)$ and $r(s, a)$ are the dynamics and reward functions. $\rho(s)$ denotes the initial state distribution. $\gamma \in (0, 1)$ denotes the discount factor. Formally, the goal is to learn a policy $\pi : \mathcal{S} \mapsto \mathcal{A}$ that maximizes cumulative discounted value function, denoted by $V^\pi(s) = \frac{1}{1-\gamma} \sum_t \mathbb{E}_{a_t \sim \pi(s_t)} [\gamma^t r(s_t, a_t) | s_0 = s]$. The Q-function of a given policy π is defined as $Q^\pi(s, a) = \frac{1}{1-\gamma} \sum_t \mathbb{E}_{a_t \sim \pi(s_t)} [\gamma^t r(s_t, a_t) | s_0 = s, a_0 = a]$, and we use Q_θ^π to denote the estimate of the Q-function of a policy π as obtained via a neural network.

Given access to an offline dataset $\mathcal{D} = \{(s, a, r, s')\}$ collected using a behavior policy π_β , we aim to first train the best possible policy and value function using the offline dataset \mathcal{D} alone, followed by an online phase that utilizes online interaction in \mathcal{M} . Our goal in this fine-tuning phase is to obtain the optimal policy with the smallest number of online samples. This can be expressed as minimizing the **cumulative regret** over rounds of online interaction: $\text{Reg}(K) := \mathbb{E}_{s \sim \rho} \sum_{t=1}^K [V^*(s) - V^{\pi^k}(s)]$. As we will demonstrate in Section 7, existing methods targeted to this setting often tend to attain regret that shrinks slowly.

Our approach will build on the conservative Q-learning (CQL) (Kumar et al., 2020) algorithm. CQL imposes an additional regularizer that penalizes the learned Q-function on out-of-distribution (OOD) actions while compensating for this pessimism on actions seen within the training dataset. Assuming that the value function is represented by a function, Q_θ , the training objective of CQL is given by

$$\min_{\theta} \underbrace{\alpha (\mathbb{E}_{s \sim \mathcal{D}, a \sim \pi} [Q_\theta(s, a)] - \mathbb{E}_{s, a \sim \mathcal{D}} [Q_\theta(s, a)])}_{\text{Conservative regularizer } \mathcal{R}(\theta)} + \frac{1}{2} \mathbb{E}_{s, a, s' \sim \mathcal{D}} [(Q_\theta(s, a) - \mathcal{B}^\pi \bar{Q}(s, a))^2], \quad (3.1)$$

where $\mathcal{B}^\pi \bar{Q}(s, a)$ is the Bellman backup operator applied to a delayed target Q-network, $\bar{Q}: \mathcal{B}^\pi \bar{Q}(s, a) := r(s, a) + \gamma \mathbb{E}_{a' \sim \pi(a'|s')} [\bar{Q}(s', a')]$. The second term is the standard TD error (Lillicrap et al., 2015; Fujimoto et al., 2018b; Haarnoja et al., 2018b). The first term $\mathcal{R}(\theta)$ (in blue) is a conservative regularizer that aims to prevent overestimation in the Q-values for OOD actions by minimizing the Q-values under the policy $\pi(a|s)$, and counterbalances by maximizing the Q-values of the actions in the dataset following the behavior policy π_β .

4. When Can Offline RL Initializations Enable Fast Online Fine-Tuning?

A natural starting point for offline pre-training and online fine-tuning is to simply initialize the value function with one that is produced by an existing offline RL method and then perform fine-tuning. However, in this section, we will show that initializations learned by many offline RL algorithms tend to perform poorly in online fine-tuning. We will study the reasons for this poor performance for the class of conservative methods to motivate our approach and then use the resulting insights to develop our method, calibrated Q-learning.

4.1. Empirical Analysis

The analysis of Nair et al. (2020b) highlights the limitations of explicit policy constraint methods for fine-tuning, therefore, in this section, we study a representative *implicit* policy constraint method, implicit Q-learning (IQL) (Kostrikov et al., 2021a) that attains good performance on benchmark tasks, and a conservative method, CQL (Kumar et al., 2020). We study the task of fine-tuning a robot policy on a visual pick-and-place task with a distractor object and sparse binary rewards, from prior work (Singh et al., 2020). More details about the offline dataset are in Appendix C.

We present the learning curves for both methods in online fine-tuning in Figure 2. While the offline Q-function initialization obtained from both methods attains a similar (normalized) return of around 0.5, neither of these methods performs well during fine-tuning: IQL improves steadily but slowly and cannot outperform CQL asymptotically. Despite the better final performance, CQL first unlearns the offline initialization and spends about 20K steps to recover before it begins to improve. This shows how neither of these approaches enables *both* a steady improvement through learning and a better asymptotic performance on the task of interest. In this work, we restrict our focus to developing effective fine-tuning strategies on top of conservative methods. Since these methods already attain good performance asymptotically but exhibit initial unlearning, we wish

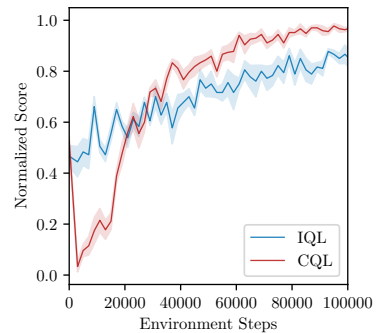


Figure 2: CQL and IQL during online fine-tuning, which begins at step 0 right after offline training. While CQL suffers from initial policy unlearning, IQL improves slowly through fine-tuning.

to now understand the potential reasons behind the initial unlearning in CQL to develop a practical approach. As a side note, we also investigate reasons that could explain the slow speed of IQL fine-tuning in Appendix E.

Why does CQL unlearn initially? To understand why this happens, we inspect the Q-values averaged over the dataset in Figure 3. Note that the Q-values learned by CQL in the offline phase are *much* smaller than their ground-truth value as expected, but these Q-values drastically jump and adjust in scale when online fine-tuning begins. In fact, we observe that performance recovery (red segment in Figure 3) *coincides* with a period where the range of Q-values changes to match the true range. This is as expected: as a conservative Q-function experiences new online data actions much worse than the offline initialization on the rollout states appears to attain higher rewards compared to the highly underestimated Q-function initialization, which in turn deceives the policy optimizer into unlearning the initial policy. We illustrate this idea visually in Figure 4. Once the Q-function has adjusted and the range of Q-values closely matches the true range, then fine-tuning can proceed normally, after recovering from the dip.

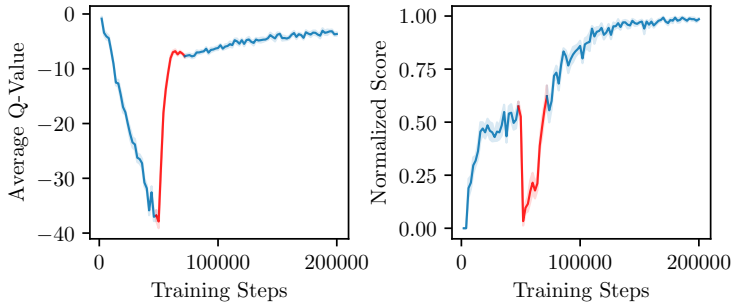


Figure 3: The evolution of the average Q-value and the success rate of CQL over the course of offline pre-training and online fine-tuning. Fine-tuning begins at 50K steps. The red-colored part denotes the period of performance recovery which also coincides with the period of Q-value adjustment.

To summarize, our empirical analysis indicates that methods such as IQL that are based on policy constraints can lead to slower asymptotic performance. Whereas conservative methods can attain good asymptotic performance, but “waste” samples to correct the learned Q-function. Thus, in this paper, we attempt to develop a good fine-tuning method that builds on top of existing conservative offline RL methods (to attain good asymptotic performance), but aims to “calibrate” the Q-function so that the initial dip in performance is avoided.

4.2. Conditions on Offline Initializations that Enable Fast Fine-Tuning

Our empirical observations from the preceding discussion motivate two conditions on the offline Q-function initialization for fast fine-tuning: **(a)** methods that learn **conservative** Q-functions can attain good asymptotic performance, and **(b)** if the Q-function is **calibrated**, (i.e., the learned Q-values closely match the range of ground-truth Q-values on the task) then online fine-tuning does not need to devote samples to unlearn and then recover the offline initialization. One approach to formalize this intuition of Q-values lying on a similar scale as the ground-truth Q-function is via the requirement that the conservative Q-values learned by the conservative offline RL method must be lower-bounded by the ground-truth Q-value of a sub-optimal reference policy. This will prevent conservatism from learning overly small Q-values. We will refer to this property as “calibration” with respect to the reference policy.

Definition 4.1 (Calibration). *An estimated Q-function Q_{θ}^{π} for a given policy π is said to be calibrated with respect to a reference policy μ if $Q_{\theta}^{\pi}(s, a) \geq Q^{\mu}(s, a), \forall (s, a) \in \mathcal{S} \times \mathcal{A}$.*

If the learned Q-function Q_{θ}^{π} is calibrated with respect to a policy μ that is worse than π , it would prevent unlearning during fine-tuning that we observed in the case of CQL. This is because the policy optimizer would not unlearn π in favor of a policy that is worse than the reference policy μ upon observing new online data as the learned Q-function Q_{θ}^{π} is constrained to be larger than Q^{μ} : $Q_{\theta}^{\pi}(s, a) \geq Q^{\mu}(s, a)$. Our practical approach Cal-QL will enforce calibration with respect to policies μ whose Q-value, $Q^{\mu}(s, a)$, can be estimated reliably (e.g., the behavior policy induced by the dataset). This is the key idea behind our method and is visually illustrated in Figure 4.

5. Cal-QL: Calibrated Q-Learning

Our approach, calibrated Q-learning (Cal-QL) learns conservative and calibrated value function initializations from an offline dataset. To this end, Cal-QL builds on CQL (Kumar et al., 2020) and then constrains the learned Q-function to produce Q-values larger than the Q-value of a reference policy μ per Definition 4.1. In principle, our approach

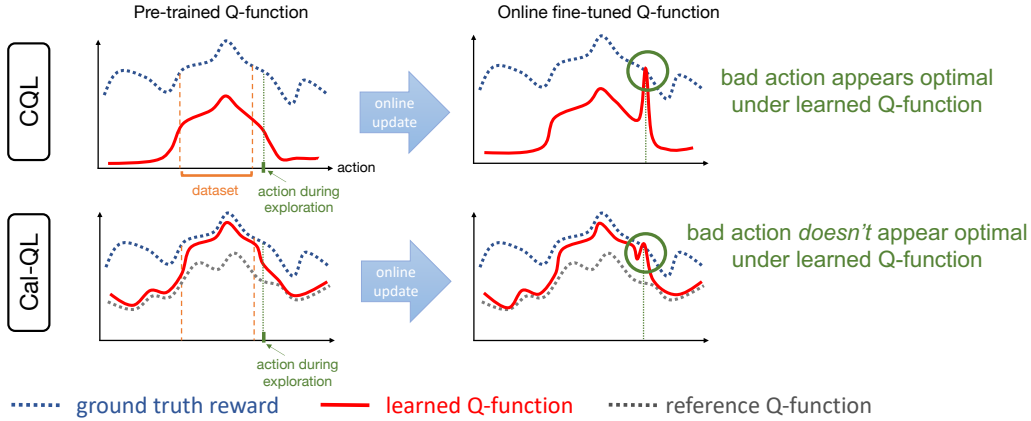


Figure 4: Intuition behind policy unlearning with CQL and the core idea behind Cal-QL. The plot visualizes a slice of the learned Q-function, ground-truth values, and reference Q-functions for a given state. Erroneous peaks centered on suboptimal actions can arise when updating CQL Q-functions with online exploration data. This in turn can lead the policy to deviate away from high-reward actions covered by the dataset in favor of erroneous unseen actions, resulting in deterioration of the pretrained policy. On the other hand, Cal-QL explicitly corrects the scale of the learned Q-values, such that actions with much worse Q-values than the reference policy do not erroneously appear optimal when updating the Q-function with additional online data.

can utilize many different choices of reference policies, but for developing a practical method, we simply utilize the behavior policy as our reference policy.

Incorporating calibration into CQL. We can constrain the learned Q-function Q_θ^π to be larger than Q^μ via a simple change to the CQL training objective shown in Equation 3.1: masking out the push down of the learned Q-value on out-of-distribution (OOD) actions in CQL if the Q-function is not calibrated, i.e., if $Q_\theta^\pi(s, a) \leq Q^\mu(s, a)$. Cal-QL modifies the CQL regularizer, $\mathcal{R}(\theta)$ in this manner:

$$\mathbb{E}_{s \sim \mathcal{D}, a \sim \pi} [\max(Q_\theta(s, a), Q^\mu(s, a))] - \mathbb{E}_{s, a \sim \mathcal{D}} [Q_\theta(s, a)], \quad (5.1)$$

where the changes from standard CQL are depicted in red. As long as α (in Equation 3.1) is large, for any state-action pair where the learned Q-value is smaller than Q^μ , the Q-function in Equation 5.1 will upper bound Q^μ in a tabular setting. Of course, as with any practical RL method, with function approximators and gradient-based optimizers, we cannot guarantee that we can enforce this condition for every state-action pair, but in our experiments, we find that Equation 5.1 is sufficient to enforce the calibration in expectation over the states in the dataset.

Pseudo-code and implementation details. Our implementation of Cal-QL directly builds on the implementation of CQL from Geng (2022). We present a pseudo-code for Cal-QL in Algorithm 1. Additionally, we list the hyperparameters α for the CQL algorithm and our baselines for each suite of tasks in Appendix D. Following the protocol in prior work (Kostrikov et al., 2021a; Song et al., 2023), the practical implementation of Cal-QL trains on a mixture of the offline data and the new online data, weighted in some proportion during fine-tuning. For estimating $Q^\mu(s, a)$, we can fit a function approximator Q_θ^μ to the return-to-go values via supervised regression, but we observed that also simply utilizing the Monte-Carlo return estimates for tasks that end in a terminal was sufficient for calibrating the learned Q-function. We show in our experiments in Section 7, how this simple *one-line* code change to the training objective drastically improves fine-tuning results compared to prior methods, while being grounded in theory.

6. Theoretical Analysis of Cal-QL

In this section, we will analyze the cumulative regret attained over the course of online fine-tuning, when the value function is pre-trained with Cal-QL, and show that enforcing both conservatism and calibration (Definition 4.1) leads to a favorable regret bound during the online phase compared to utilizing naïve uncalibrated conservative methods. Our analysis utilizes tools from Song et al. (2023), but analyzes a different algorithm that runs conservative offline RL with calibration for offline training and online fine-tuning.

Notation & terminology. In our analysis, we will consider an idealized version of Cal-QL for simplicity. Specifically, following prior work (Song et al., 2023), we will operate in a finite-horizon setting with a horizon H . We denote the learned Q-function at each learning iteration k for a given (s, a) pair and time-step h by $Q_\theta^k(s, a)$. For any given policy π , let $C_\pi \geq 1$ denote the concentrability coefficient such that $C_\pi := \max_{f \in \mathcal{C}} \frac{\sum_{h=0}^{H-1} \mathbb{E}_{s, a \sim \pi} [\mathcal{T} f_{h+1}(s, a) - f_h(s, a)]}{\sqrt{\sum_{h=0}^{H-1} \mathbb{E}_{s, a \sim \pi} (\mathcal{T} f_{h+1}(s, a) - f_h(s, a))^2}}$, i.e.,

a coefficient that quantifies the distribution shift between the policy π and the dataset \mathcal{D} , in terms of the ratio of Bellman errors averaged under π and the dataset \mathcal{D} . Note that \mathcal{C} represents the Q-function class and we assume \mathcal{C} has a bellman-bilinear rank (Du et al., 2021) of d . We also use C_π^μ to denote the concentrability coefficient over a subset

of the Q-function class induced by a reference policy μ : $C_\pi^{\text{ref}} := \max_{f \in \mathcal{C}, f(s,a) \geq Q^{\text{ref}}(s,a)} \frac{\sum_{h=0}^{H-1} \mathbb{E}_{s,a \sim d_h^\pi} [\mathcal{T} f_{h+1}(s,a) - f_h(s,a)]}{\sqrt{\sum_{h=0}^{H-1} \mathbb{E}_{s,a \sim \nu_h} (\mathcal{T} f_{h+1}(s,a) - f_h(s,a))^2}}$,

which intuitively provides $C_\pi^\mu \leq C_\pi$. Similar to \mathcal{C} , let d_μ denote the bellman bilinear rank of \mathcal{C}_μ – the Q-function class w.r.t. the all policies μ . Intuitively, we have $\mathcal{C}_\mu \subset \mathcal{C}$, which implies that $d_\mu \leq d$. The formal definitions are provided in Appendix B.2. We will use π^k to denote the arg-max policy induced by Q_θ^k .

6.1. Intuition

We first intuitively discuss how calibration and conservatism enable Cal-QL to attain a smaller regret compared to not imposing either condition. Recall that our goal is to bound the cumulative regret of online fine-tuning, $\sum_t \mathbb{E}_{s_0 \sim \rho} [V^{\pi^*}(s_0) - V^{\pi^k}(s_0)]$. We can decompose this expression of regret into two terms:

$$\text{Reg}(K) = \underbrace{\sum_{k=1}^K \mathbb{E}_{s_0 \sim \rho} \left[V^*(s_0) - \max_a Q_\theta^k(s_0, a) \right]}_{(i) := \text{miscalibration}} + \underbrace{\sum_{k=1}^K \mathbb{E}_{s_0 \sim \rho} \left[\max_a Q_\theta^k(s_0, a) - V^{\pi^k}(s_0) \right]}_{(ii) := \text{optimism}}. \quad (6.1)$$

This decomposition of regret into terms (i) and (ii) is instructive. Term (ii) corresponds to the amount of over-estimation in the learned value function, which is expected to be small if a conservative RL algorithm is used for training. Term (i) is the difference between the ground-truth value of the optimal policy and the learned Q-function and is negative if the learned Q-function were calibrated against the optimal policy (per Definition 4.1). Of course, this is not always possible because we do not know V^* a priori. But note that when Cal-QL utilizes a reference policy μ with a high value V^μ , close to V^* , then the learned Q-function Q_θ is calibrated with respect to Q^μ per Condition 4.1 and term (i) can still be controlled. Therefore, controlling this regret requires striking a balance between learning a calibrated (term (i)) and conservative (term (ii)) Q-function. We now formalize this intuition and defer the detailed proof to Appendix B.4.

6.2. Theorem Statement

Theorem 6.1 (Informal regret bound of Cal-QL). *With high probability, Cal-QL obtains the following bound on total regret accumulated during online fine-tuning:*

$$\text{Reg}(K) = \tilde{O} \left(\min \left\{ C_{\pi^*}^\mu H \sqrt{dK \log(|\mathcal{F}|)}, KE_\rho[V^*(s_0) - V^\mu(s_0)] + H \sqrt{d_\mu K \log(|\mathcal{F}|)} \right\} \right),$$

where \mathcal{F} is the functional class of the Q-function.

Comparison to Song et al. (2023). Song et al. (2023) analyzes an online RL algorithm that utilizes offline data without imposing conservatism or calibration. We now compare Theorem 6.1 to Theorem 1 of Song et al. (2023) to understand the impact of these conditions on the final regret guarantee. Theorem 1 of Song et al. (2023) presents a regret bound: $\text{Reg}(K) = \tilde{O} \left(C_{\pi^*} H \sqrt{dK \log(|\mathcal{F}|)} \right)$ and we note some improvements in our guarantee, that we also verify via experiments in Section 7.3: **(a)** for the setting where the reference policy μ contains near-optimal behavior, i.e., $V^* - V^\mu \lesssim O(H \sqrt{d \log(|\mathcal{F}|)}/K)$, then Cal-QL can enable a tighter regret guarantee compared to Song et al. (2023); **(b)** as we show in Appendix B.3, the concentrability coefficient $C_{\pi^*}^\mu$ appearing in our guarantee is no larger than the one that appears in Theorem 1 of Song et al. (2023), providing another source of improvement; and **(c)** finally, in the worst possible case, where the reference policy has broad coverage and is highly sub-optimal, Cal-QL reverts back to the guarantee from Song et al. (2023), meaning that Cal-QL is not any worse in this case.

7. Experimental Evaluation

The goal of our experimental evaluation is to study how well Cal-QL can facilitate sample-efficient online fine-tuning. To this end, we study the performance of Cal-QL in comparison with several other state-of-the-art fine-tuning methods on a variety of offline RL benchmark tasks from D4RL (Fu et al., 2020), Singh et al. (2020), and Nair et al. (2020b), evaluating performance before and after online fine-tuning. We also study the effectiveness of Cal-QL on higher-dimensional tasks, where the policy and value function must process raw image observations. Finally, we perform several empirical studies to understand the efficacy of Cal-QL with different dataset compositions and to understand the impact of errors in reference function value estimation on Cal-QL.

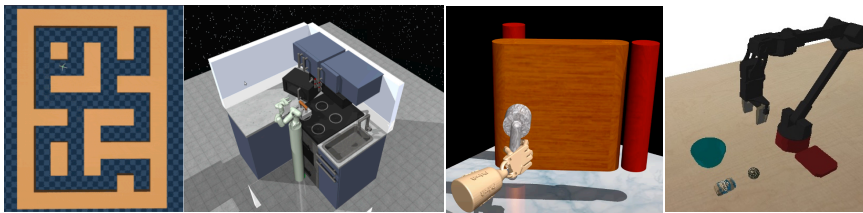


Figure 5: Tasks: We evaluate Cal-QL on a diverse set of benchmark problems: AntMaze and FrankaKitchen domains from Fu et al. (2020), Adroit tasks from Nair et al. (2020b) and a vision-based robotic manipulation task from Kumar et al. (2022).

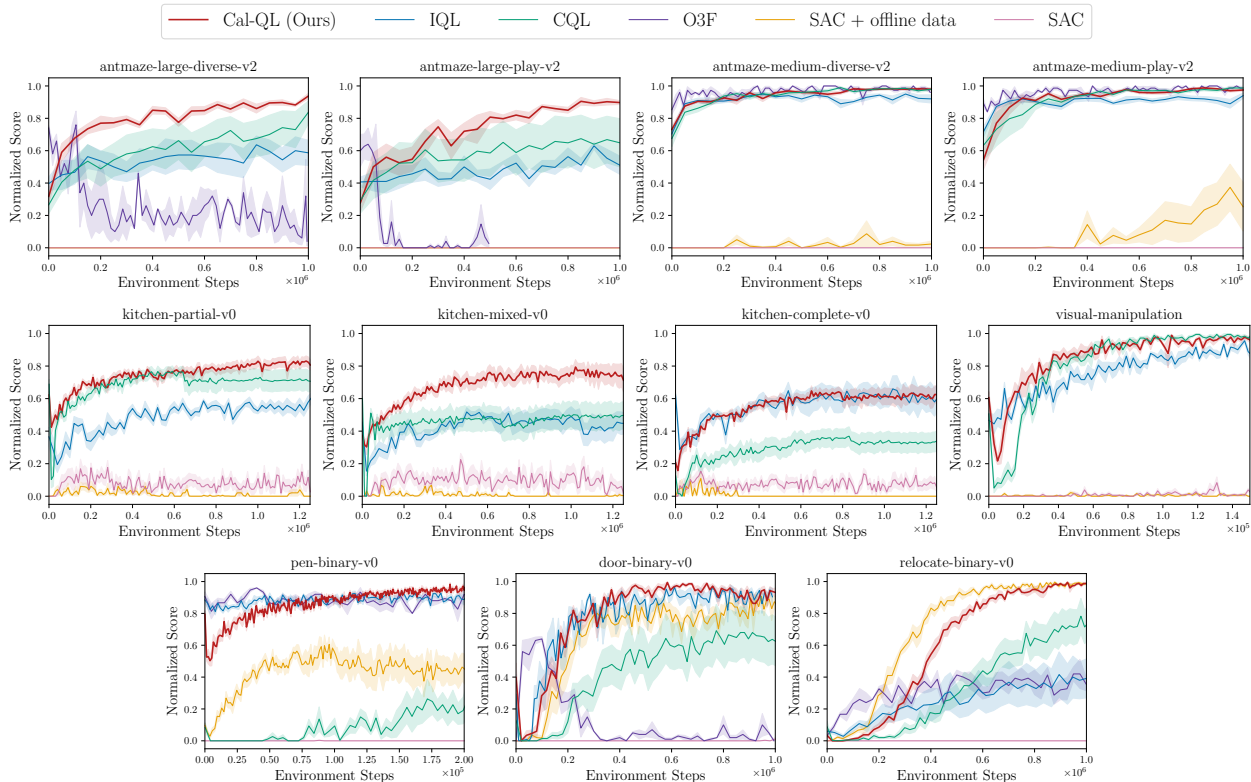


Figure 6: Online fine-tuning after offline initialization on the benchmark tasks. The plots show the online fine-tuning phase *after* pre-training for each method (except SAC-based approaches which are not pre-trained). We use at least 6 seeds for each method. Observe that Cal-QL consistently matches or exceeds the speed and final performance of the best prior method and is the only algorithm to do so across all tasks.

Offline RL tasks and datasets. We evaluate Cal-QL on a number of benchmark tasks and datasets used by prior works (Kostrikov et al., 2021a; Nair et al., 2020b) to evaluate fine-tuning performance: (1) The AntMaze tasks from D4RL (Fu et al., 2020) that require controlling an 8-DoF ant quadruped robot to navigate from a starting point to a desired goal location in a maze. The reward is +1 if the agent reaches within a pre-specified small radius around the goal and 0 otherwise. We consider two kinds of maze layouts (medium and large mazes from Fu et al. (2020)) and two data compositions: **play** and **diverse** that vary in coverage of actions at different regions of the state space and sub-optimality of the behavior policy. (2) The FrankaKitchen tasks from D4RL require controlling a 9-DoF Franka robot to attain a desired configuration of a kitchen. To succeed, a policy must complete four sub-tasks in the kitchen within a single rollout, and it receives a binary reward of +1/0 for every sub-task it completes. (3) Three Adroit dexterous manipulation tasks (Rajswaran et al., 2018; Kostrikov et al., 2021a; Nair et al., 2020b) that require learning complex manipulation skills on a 28-DoF five-fingered hand to (a) manipulate a pen in-hand to a desired configuration (pen-binary), (b) open a door by unlatching the handle (door-binary), and (c) relocating a ball to a desired location (relocate-binary). An agent obtains a sparse binary +1/0 reward if it succeeds in solving the task. Each of these tasks only provides an extremely narrow offline dataset consisting of 25 demonstrations collected via human teleoperation and additional trajectories collected by a BC policy. Finally, to evaluate the efficacy of Cal-QL on more challenging tasks where we must learn from raw visual observations, we study (4) a pick-and-place task from prior work (Singh et al., 2020; Kumar et al., 2022) that requires learning to pick a ball and place it in a bowl, in the presence of distractors.

Comparisons, prior methods, and evaluation protocol. We compare Cal-QL to running online SAC (Haarnoja et al., 2018c) from scratch, as well as prior approaches that leverage offline data. This includes naively fine-tuning offline RL methods such as CQL (Kumar et al., 2020) and IQL (Kostrikov et al., 2021a), as well as fine-tuning with O3F (Mark et al., 2022), a method specifically designed for offline RL training followed by online fine-tuning. In addition, we also compare to a baseline that trains SAC (Haarnoja et al., 2018c) using both online data and offline data (denoted by “SAC + offline data”). This simple and pragmatic approach most closely matches DDPGfD (Vecerik et al., 2017), updated to use the stronger online off-policy RL algorithm (SAC). Note that in contrast to DDPGfD, we are using the offline data provided in each benchmark task, which is *not necessarily demonstration* data. We present learning curves for online fine-tuning and also quantitatively evaluate each method on its ability to improve the initialization learned from offline data measured in terms of final performance after a pre-defined number of steps per domain and the cumulative regret accumulated over the course of online fine-tuning. In Section 7.2, we also compare Cal-QL to a more recent approach, RLPD (Ball et al., 2023), a more sample-efficient version of “SAC + offline data”.

7.1. Empirical Results

We first present a comparison of Cal-QL in terms of the normalized performance before and after fine-tuning in Table 1 and the cumulative regret accumulated in a fixed number of steps of environment interaction in Table 2. Following the protocol of Fu et al. (2020), we normalize the average return values for each domain with respect to the highest possible return (+4 in FrankaKitchen; +1 in other tasks; see Appendix D.1 for more details).

Cal-QL improves the offline initialization significantly. Observe in Table 1 and Figure 6 that while the performance of offline initialization acquired by Cal-QL performs about comparably (or slightly worse) to the initialization acquired by other methods such as IQL, Cal-QL is able to improve over its offline initialization by over **2x** outperforming the next best method (IQL) on **10 out of 11** tasks, by about **27%** in terms of aggregate performance.

Cal-QL enables fast fine-tuning. To understand the efficacy of Cal-QL in enabling learning quickly during online fine-tuning, we measure the cumulative regret accumulated over the course of fine-tuning. Observe in Table 2 that Cal-QL consistently achieves a smaller regret of 0.22 on **8 out of 11** tasks, improving over the next best method by **41%**. Intuitively, this means that Cal-QL does not require actively collecting data from highly sub-optimal policies. In tasks such as `relocate-binary`, Cal-QL enjoys the fast online learning benefits associated with naïve online RL methods that incorporate the offline data in the replay buffer (SAC + offline data and Cal-QL are the only two methods to attain a score of $\geq 99\%$ on this task) unlike prior offline RL methods such as IQL. As shown in Figure 6, in the `kitchen` and `antmaze` domains, Cal-QL brings the benefits of fast online learning together with a good offline initialization, improving drastically on the regret metric. Finally, observe that the initial unlearning at the beginning of fine-tuning with conservative methods observed in Section 4.1 is greatly alleviated in all tasks.

Domain	Task	IQL	CQL	SAC + offline data	SAC	O3F	Cal-QL (Ours)
antmaze	large-diverse	0.40 → 0.59	0.27 → 0.84	0.00 → 0.00	0.00 → 0.00	0.74 → 0.04	0.32 → 0.94
	large-play	0.41 → 0.51	0.29 → 0.65	0.00 → 0.00	0.00 → 0.00	0.60 → 0.03	0.28 → 0.90
	medium-diverse	0.70 → 0.92	0.68 → 0.98	0.00 → 0.02	0.00 → 0.00	0.85 → 0.96	0.73 → 0.98
	medium-play	0.72 → 0.94	0.63 → 0.99	0.00 → 0.25	0.00 → 0.00	0.89 → 0.99	0.54 → 0.98
kitchen	partial	0.37 → 0.61	0.69 → 0.71	0.00 → 0.00	0.00 → 0.03	N/A → N/A	0.62 → 0.81
	mixed	0.46 → 0.45	0.60 → 0.50	0.00 → 0.00	0.00 → 0.02	N/A → N/A	0.37 → 0.71
	complete	0.62 → 0.62	0.12 → 0.34	0.00 → 0.00	0.00 → 0.05	N/A → N/A	0.20 → 0.62
adroit	pen-binary	0.88 → 0.89	0.08 → 0.19	0.10 → 0.45	0.00 → 0.00	0.91 → 0.92	0.79 → 0.96
	door-binary	0.29 → 0.87	0.13 → 0.62	0.00 → 0.86	0.00 → 0.01	0.00 → 0.00	0.40 → 0.90
	relocate-binary	0.04 → 0.37	0.09 → 0.75	0.00 → 0.99	0.01 → 0.24	0.03 → 0.35	0.03 → 0.99
COG	manipulation	0.47 → 0.89	0.51 → 0.97	0.00 → 0.00	0.00 → 0.04	N/A → N/A	0.61 → 0.97
	average	0.49 → 0.70 (+ 42.9%)	0.37 → 0.69 (+ 84.4%)	N/A → 0.23	N/A → 0.04	0.57 → 0.47 (- 18.2%)	0.44 → 0.89 (+ 99.6%)

Table 1: Normalized score before and after the online fine-tuning. We trained each method for 1M environment steps on `antmaze`, `door-binary`, and `relocate-binary` tasks, 200K steps on `pen-binary`, 1.25M steps on `kitchen` tasks, and 1.5M steps on `visual-manipulation`. Observe that Cal-QL improves over the best prior fine-tuning method and attains a much larger performance improvement over the course of online fine-tuning.

7.2. Cal-QL With High Update-to-Data (UTD) Ratio

While Cal-QL enabled effective fine-tuning by a single gradient step for each environment step, we can further enhance online sample efficiency by increasing the number of gradient steps per environment step made by the algorithm. The number of updates per environment step is usually called the update-to-data (UTD) ratio. We will now evaluate Cal-QL with a high UTD ratio. In Figure 7, we present the performance of Cal-QL with UTD = 5 on the `visual-manipulation` task. We can see that Cal-QL can achieve higher sample efficiency by using UTD = 5, and the initial unlearning disappears completely which we studied previously in Section 4.1. Interestingly, while prior fine-tuning methods such as IQL do not improve with a higher UTD (see Figure 7), Cal-QL and CQL benefit from using a higher UTD ratio. We will further discuss this in Appendix E.

We noticed that simply running Cal-QL with an even higher UTD value (e.g., 20) leads to previously-observed challenges pertaining to overfitting (Li et al., 2023; Chen et al., 2021; Ball et al., 2023; D’Oro et al., 2023). To address

Task	IQL	CQL	SAC+od	SAC	O3F	Cal-QL
large-diverse	0.46	0.39	1.00	1.00	0.75	0.21
large-play	0.52	0.43	1.00	1.00	0.88	0.27
medium-diverse	0.09	0.06	0.98	1.00	0.03	0.06
medium-play	0.10	0.08	0.90	1.00	0.04	0.08
partial	0.51	0.32	0.99	0.92	N/A	0.26
mixed	0.58	0.54	0.99	0.91	N/A	0.32
complete	0.44	0.71	0.99	0.93	N/A	0.44
pen-binary	0.12	0.92	0.56	1.00	0.12	0.12
door-binary	0.24	0.53	0.30	1.00	0.87	0.17
relocate-binary	0.75	0.65	0.20	0.75	0.69	0.31
visual-manipulation	0.24	0.19	1.00	0.99	N/A	0.15
average	0.37	0.44	0.81	0.95	0.48	0.22

Table 2: Cumulative regret averaged over the steps of online fine-tuning. The smaller the better, worst case is 1.00. Note that Cal-QL attains the smallest regret in aggregate, improving over the best prior method in 8 out of 11 tasks that we study.

these challenges in high UTD settings, we ran Cal-QL in conjunction with the Q-function architecture in Ball et al. (2023) (i.e., we utilized layer normalization in the Q-function and ensemble backups akin to Chen et al. (2021)) to prevent overfitting. Note that Cal-QL still first pre-trains on the offline dataset using Equation 5.1 followed by online fine-tuning, unlike RLPD that runs online RL from scratch on offline and online data.

In Figure 8, we compare Cal-QL (UTD = 20) with RLPD (Ball et al., 2023) (UTD = 20) and also Cal-QL (UTD = 1) as a baseline. Observe that Cal-QL (UTD = 20) improves over Cal-QL (UTD = 1) and training from scratch (RLPD).

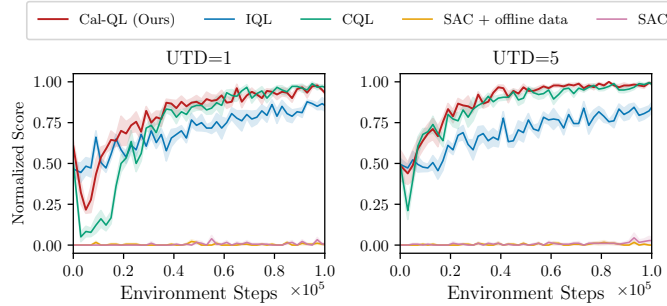


Figure 7: UTD ablation: We observe that using a higher UTD ratio can lead to higher sample efficiency for Cal-QL and CQL but not for IQL.

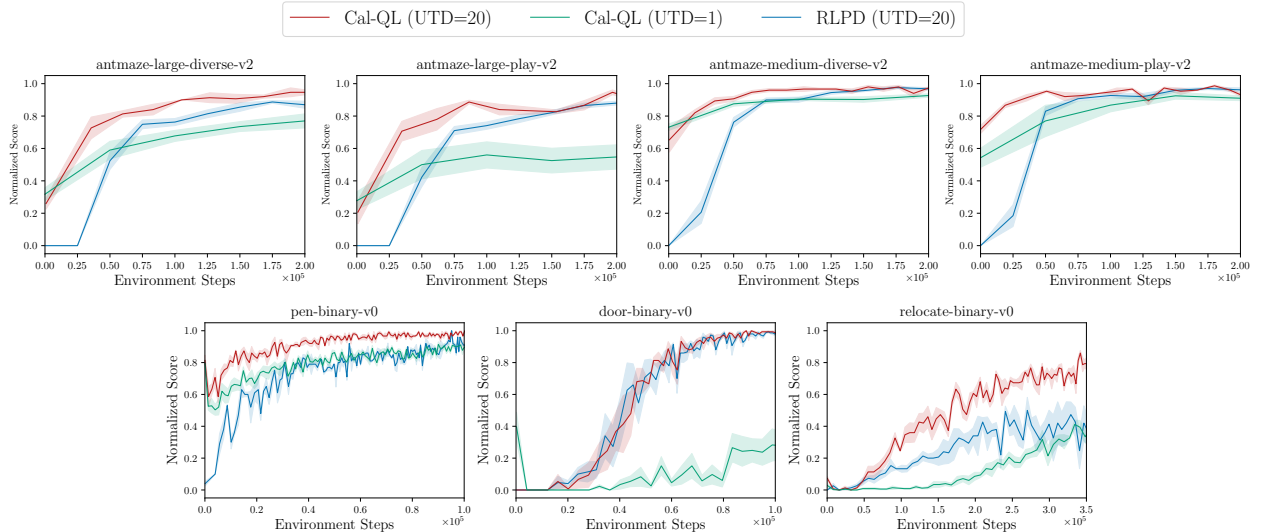


Figure 8: Cal-QL with UTD=20. Incorporating design choices from RLPD enables Cal-QL to achieve sample-efficient fine-tuning with UTD=20. Specifically, Cal-QL generally attains similar or higher asymptotic performance as RLPD, while also exhibiting a smaller cumulative regret.

7.3. Understanding the Behavior of Cal-QL

In this section, we aim to understand the behavior of Cal-QL by performing controlled experiments that modify the dataset composition, and by investigating various metrics to understand the properties of scenarios where utilizing Cal-QL is especially important.

Effect of data composition. To understand the efficacy of Cal-QL with different data compositions, we ran it on a newly constructed fine-tuning task on the medium-size AntMaze domain with a low-coverage offline dataset, which is generated via a scripted controller that starts from a fixed initial position and navigates the ant to a fixed goal position. In Figure 9, we plot the performance of Cal-QL and baseline CQL (for comparison) on this task, alongside the trend of average Q-values over the course of offline pre-training (to the left of the dashed vertical line, before 250 training epochs) and online fine-tuning (to the right of the vertical dashed line, after 250 training epochs), and the trend of *bounding rate*, i.e., the fraction of transitions in the data-buffer for which the constraint in Cal-QL actively lower-bounds the learned Q-function with the reference Q-value. For comparison, we also plot these quantities for a diverse dataset with high coverage on the task (we use the `antmaze-medium-diverse` from Fu et al. (2020) as a representative diverse dataset) in Figure 9.

Observe that for the diverse dataset, both naïve CQL and Cal-QL perform similarly, and indeed, the learned Q-values behave similarly for both of these methods. In this setting, online learning doesn’t spend samples to correct the Q-function when fine-tuning begins leading to a low bounding rate, almost always close to 0. Instead, with the narrow dataset, we observe that the Q-values learned by naïve CQL are much smaller, and are corrected once fine-tuning begins. This correction co-occurs with a drop in performance (solid blue line on left), and naïve CQL is unable to recover from this drop. Cal-QL which calibrates the scale of the Q-function for many more samples in the dataset, stably transitions to online fine-tuning with no unlearning (solid red line on left).

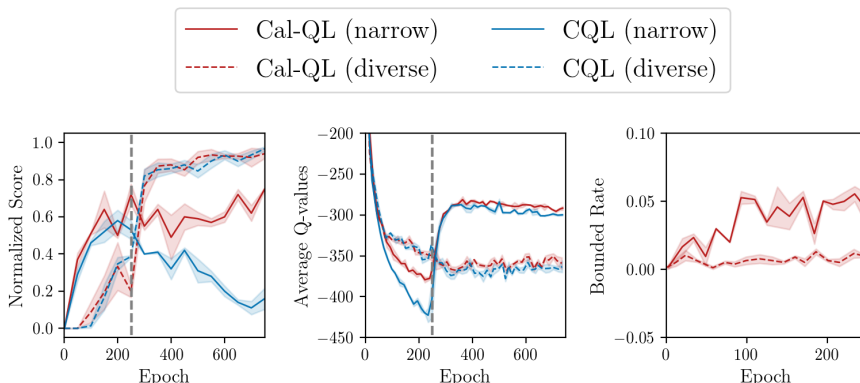


Figure 9: Performance of Cal-QL with different data compositions. Cal-QL is most effective with narrow datasets, where Q-values need to be corrected at the beginning of fine-tuning.

The study reveals the behavior of Cal-QL: in settings with narrow datasets (e.g., in the experiment above and in the `adroit` and `visual-manipulation` domains from Figure 6), Q-values learned by naïve conservative methods are more likely to be smaller than the ground-truth Q-function of the behavior policy due to function approximation errors. Hence utilizing Cal-QL to calibrate the Q-function against the behavior policy can be significantly helpful. On the other hand, with significantly high-coverage datasets, especially in problems where the behavior policy is also random and sub-optimal, Q-values learned by naïve methods are likely to already be calibrated with respect to those of the behavior policy. Therefore no explicit calibration might be needed (and indeed, the bounding rate tends to be very close to 0 as shown in Figure 9). In this case, Cal-QL will revert back to standard CQL, as we observe in the case of the diverse dataset above. This intuition is also reflected in Theorem 6.1: when the reference policy μ is close to a narrow, expert policy, we would expect Cal-QL to be especially effective in controlling the efficiency of online fine-tuning.

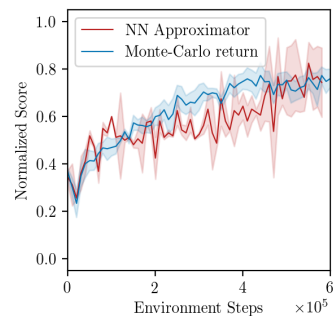


Figure 10: The performance of Cal-QL using a neural net approximator for the reference value function is comparable to using the Monte-Carlo return.

Estimation errors in the reference value function do not affect performance significantly. In our experiments, we compute the reference value functions using Monte-Carlo return estimates. However, this may not be available in all tasks. How does Cal-QL behave when reference value functions must be estimated using the offline dataset itself? To answer this, we ran an experiment on the `kitchen` domain, where instead of using an estimate for Q^μ based on the Monte-Carlo return, we train a neural network function approximator Q_θ^μ to approximate Q^μ via supervised regression on to Monte-Carlo return, which is then utilized by Cal-QL. Observe in Figure 10, that the performance of Cal-QL largely remains unaltered. This implies as long as we can obtain a reasonable function approximator to estimate the Q-function of the reference policy (in this case, the behavior policy), errors in the reference Q-function do not affect the performance of Cal-QL significantly.

8. Discussion

In this work we developed Cal-QL a method for acquiring offline initializations that facilitate fast online fine-tuning. Cal-QL learns conservative value functions but additionally constrains to be larger than the value function of a reference policy. This form of calibration of the Q-function allows us to avoid initial unlearning in online fine-tuning with conservative methods, while also retaining effective asymptotic performance that these methods typically exhibit. Our theoretical and experimental results highlight the benefit of Cal-QL in enabling fast online fine-tuning. While Cal-QL outperforms prior methods, we believe there is a scope for developing even more practically effective methods by carefully adjusting calibration and conservatism (see Theorem 6.1). Another interesting direction for future work is to extend Cal-QL to settings with different pre-training and fine-tuning tasks that appear in real-world problems.

Acknowledgments

This research was partially supported by the Office of Naval Research N00014-21-1-2838, N00014-22-1-2102, ARO W911NF-21-1-0097, the joint Simons Foundation-NSF DMS grant #2031899, AFOSR FA9550-22-1-0273, and Tsinghua-Berkeley Shenzhen Institute (TBSI) Research Fund, as well as support from Intel and C3.ai, the Savio computational cluster resource provided by the Berkeley Research Computing program, and computing support from Google. We thank Philip J. Ball, Laura Smith, and Ilya Kostrikov for sharing the experimental results of RLPD. AK is supported by the Apple Scholars in AI/ML PhD Fellowship. MN is partially supported by the Nakajima Foundation Overseas Fellowship. YZ is partially supported by Siemens CITRIS and TBSI research fund. YZ would like to thank Song Mei for insightful suggestions on the presentation of Theorem 6.1.

References

- Anurag Ajay, Aviral Kumar, Pulkit Agrawal, Sergey Levine, and Ofir Nachum. Opal: Offline primitive discovery for accelerating offline reinforcement learning. *arXiv preprint arXiv:2010.13611*, 2020.
- Philip J Ball, Laura Smith, Ilya Kostrikov, and Sergey Levine. Efficient online reinforcement learning with offline data. *arXiv preprint arXiv:2302.02948*, 2023.
- Alex Beeson and Giovanni Montana. Improving td3-bc: Relaxed policy constraint for offline learning and stable online fine-tuning. *arXiv preprint arXiv:2211.11802*, 2022.
- Jacob Buckman, Carles Gelada, and Marc G Bellemare. The importance of pessimism in fixed-dataset policy optimization. *arXiv preprint arXiv:2009.06799*, 2020.
- Xinyue Chen, Che Wang, Zijian Zhou, and Keith W. Ross. Randomized ensembled double q-learning: Learning fast without a model. In *International Conference on Learning Representations*, 2021. URL <https://openreview.net/forum?id=AY8zfZm0tDd>.
- Ching-An Cheng, Tengyang Xie, Nan Jiang, and Alekh Agarwal. Adversarially trained actor critic for offline reinforcement learning. *arXiv preprint arXiv:2202.02446*, 2022.
- Jacob Devlin, Ming-Wei Chang, Kenton Lee, and Kristina Toutanova. Bert: Pre-training of deep bidirectional transformers for language understanding. *arXiv preprint arXiv:1810.04805*, 2018.
- Pierluca D’Oro, Max Schwarzer, Evgenii Nikishin, Pierre-Luc Bacon, Marc G Bellemare, and Aaron Courville. Sample-efficient reinforcement learning by breaking the replay ratio barrier. In *The Eleventh International Conference on Learning Representations*, 2023. URL <https://openreview.net/forum?id=OpC-9aBBVJe>.
- Simon Du, Sham Kakade, Jason Lee, Shachar Lovett, Gaurav Mahajan, Wen Sun, and Ruosong Wang. Bilinear classes: A structural framework for provable generalization in rl. In *International Conference on Machine Learning*, pages 2826–2836. PMLR, 2021.
- Justin Fu, Aviral Kumar, Ofir Nachum, George Tucker, and Sergey Levine. D4rl: Datasets for deep data-driven reinforcement learning. *arXiv preprint arXiv:2004.07219*, 2020.
- Scott Fujimoto, David Meger, and Doina Precup. Off-policy deep reinforcement learning without exploration. *arXiv preprint arXiv:1812.02900*, 2018a.
- Scott Fujimoto, Herke van Hoof, and David Meger. Addressing function approximation error in actor-critic methods. In *International Conference on Machine Learning (ICML)*, pages 1587–1596, 2018b.

- Xinyang Geng. Jaxcql: a simple implementation of sac and cql in jax. 2022. URL <https://github.com/young-geng/JaxCQL>.
- Seyed Kamyar Seyed Ghasemipour, Dale Schuurmans, and Shixiang Shane Gu. Emaq: Expected-max q-learning operator for simple yet effective offline and online rl. In *International Conference on Machine Learning*, pages 3682–3691. PMLR, 2021.
- Yijie Guo, Shengyu Feng, Nicolas Le Roux, Ed Chi, Honglak Lee, and Minmin Chen. Batch reinforcement learning through continuation method. In *International Conference on Learning Representations*, 2020.
- Abhishek Gupta, Vikash Kumar, Corey Lynch, Sergey Levine, and Karol Hausman. Relay policy learning: Solving long-horizon tasks via imitation and reinforcement learning. *arXiv preprint arXiv:1910.11956*, 2019.
- Abhishek Gupta, Aldo Pacchiano, Yuexiang Zhai, Sham M Kakade, and Sergey Levine. Unpacking reward shaping: Understanding the benefits of reward engineering on sample complexity. *arXiv preprint arXiv:2210.09579*, 2022.
- T. Haarnoja, A. Zhou, P. Abbeel, and S. Levine. Soft actor-critic: Off-policy maximum entropy deep reinforcement learning with a stochastic actor. In *arXiv*, 2018a. URL <https://arxiv.org/pdf/1801.01290.pdf>.
- Tuomas Haarnoja, Aurick Zhou, Kristian Hartikainen, George Tucker, Sehoon Ha, Jie Tan, Vikash Kumar, Henry Zhu, Abhishek Gupta, Pieter Abbeel, and Sergey Levine. Soft actor-critic algorithms and applications. Technical report, 2018b.
- Tuomas Haarnoja, Aurick Zhou, Kristian Hartikainen, George Tucker, Sehoon Ha, Jie Tan, Vikash Kumar, Henry Zhu, Abhishek Gupta, Pieter Abbeel, et al. Soft actor-critic algorithms and applications. *arXiv preprint arXiv:1812.05905*, 2018c.
- Kaiming He, Xinlei Chen, Saining Xie, Yanghao Li, Piotr Dollár, and Ross Girshick. Masked autoencoders are scalable vision learners. In *Proceedings of the IEEE/CVF Conference on Computer Vision and Pattern Recognition*, pages 16000–16009, 2022.
- Todd Hester, Matej Vecerik, Olivier Pietquin, Marc Lanctot, Tom Schaul, Bilal Piot, Dan Horgan, John Quan, Andrew Sendonaris, Ian Osband, et al. Deep q-learning from demonstrations. In *Thirty-Second AAAI Conference on Artificial Intelligence*, 2018.
- Chi Jin, Qinghua Liu, and Sobhan Miryoosefi. Bellman eluder dimension: New rich classes of rl problems, and sample-efficient algorithms. *Advances in neural information processing systems*, 34:13406–13418, 2021a.
- Ying Jin, Zhuoran Yang, and Zhaoran Wang. Is pessimism provably efficient for offline rl? In *International Conference on Machine Learning*, pages 5084–5096. PMLR, 2021b.
- Sham Kakade and John Langford. Approximately optimal approximate reinforcement learning. In *International Conference on Machine Learning (ICML)*, volume 2, 2002.
- Bingyi Kang, Zequn Jie, and Jiashi Feng. Policy optimization with demonstrations. In *International conference on machine learning*, pages 2469–2478. PMLR, 2018.
- Rahul Kidambi, Aravind Rajeswaran, Praneeth Netrapalli, and Thorsten Joachims. Morel: Model-based offline reinforcement learning. *arXiv preprint arXiv:2005.05951*, 2020.
- Ilya Kostrikov, Ashvin Nair, and Sergey Levine. Offline reinforcement learning with implicit q-learning. *arXiv preprint arXiv:2110.06169*, 2021a.
- Ilya Kostrikov, Jonathan Tompson, Rob Fergus, and Ofir Nachum. Offline reinforcement learning with fisher divergence critic regularization. *arXiv preprint arXiv:2103.08050*, 2021b.
- Aviral Kumar, Aurick Zhou, George Tucker, and Sergey Levine. Conservative q-learning for offline reinforcement learning. *arXiv preprint arXiv:2006.04779*, 2020.
- Aviral Kumar, Anikait Singh, Frederik Ebert, Yanlai Yang, Chelsea Finn, and Sergey Levine. Pre-Training for Robots: Offline RL Enables Learning New Tasks from a Handful of Trials. *arXiv e-prints*, art. arXiv:2210.05178, October 2022. doi: 10.48550/arXiv.2210.05178.
- Aviral Kumar, Anikait Singh, Frederik Ebert, Yanlai Yang, Chelsea Finn, and Sergey Levine. Pre-training for robots: Offline rl enables learning new tasks from a handful of trials. *arXiv preprint arXiv:2210.05178*, 2022.

- Seunghyun Lee, Younggyo Seo, Kimin Lee, Pieter Abbeel, and Jinwoo Shin. Offline-to-online reinforcement learning via balanced replay and pessimistic q-ensemble. In *Conference on Robot Learning*, pages 1702–1712. PMLR, 2022.
- Sergey Levine, Aviral Kumar, George Tucker, and Justin Fu. Offline reinforcement learning: Tutorial, review, and perspectives on open problems. *arXiv preprint arXiv:2005.01643*, 2020.
- Gen Li, Yuting Wei, Yuejie Chi, Yuantao Gu, and Yuxin Chen. Breaking the sample size barrier in model-based reinforcement learning with a generative model. *arXiv preprint arXiv:2005.12900*, 2020.
- Qiyang Li, Yuexiang Zhai, Yi Ma, and Sergey Levine. Understanding the complexity gains of single-task rl with a curriculum. *arXiv preprint arXiv:2212.12809*, 2022.
- Qiyang Li, Aviral Kumar, Ilya Kostrikov, and Sergey Levine. Efficient deep reinforcement learning requires regulating overfitting. In *The Eleventh International Conference on Learning Representations*, 2023. URL <https://openreview.net/forum?id=14-kr46GvP->.
- Timothy P Lillicrap, Jonathan J Hunt, Alexander Pritzel, Nicolas Heess, Tom Erez, Yuval Tassa, David Silver, and Daan Wierstra. Continuous control with deep reinforcement learning. *arXiv preprint arXiv:1509.02971*, 2015.
- Jiafei Lyu, Xiaoteng Ma, Xiu Li, and Zongqing Lu. Mildly conservative q-learning for offline reinforcement learning. *arXiv preprint arXiv:2206.04745*, 2022.
- Max Sobol Mark, Ali Ghadirzadeh, Xi Chen, and Chelsea Finn. Fine-tuning offline policies with optimistic action selection. In *Deep Reinforcement Learning Workshop NeurIPS 2022*, 2022.
- Ofir Nachum, Bo Dai, Ilya Kostrikov, Yinlam Chow, Lihong Li, and Dale Schuurmans. Algaedice: Policy gradient from arbitrary experience. *arXiv preprint arXiv:1912.02074*, 2019.
- Ashvin Nair, Murtaza Dalal, Abhishek Gupta, and Sergey Levine. Accelerating online reinforcement learning with offline datasets. *CoRR*, abs/2006.09359, 2020a. URL <https://arxiv.org/abs/2006.09359>.
- Ashvin Nair, Murtaza Dalal, Abhishek Gupta, and Sergey Levine. Accelerating online reinforcement learning with offline datasets. *arXiv preprint arXiv:2006.09359*, 2020b.
- Aravind Rajeswaran, Vikash Kumar, Abhishek Gupta, Giulia Vezzani, John Schulman, Emanuel Todorov, and Sergey Levine. Learning complex dexterous manipulation with deep reinforcement learning and demonstrations. *arXiv preprint arXiv:1709.10087*, 2017.
- Aravind Rajeswaran, Vikash Kumar, Abhishek Gupta, Giulia Vezzani, John Schulman, Emanuel Todorov, and Sergey Levine. Learning complex dexterous manipulation with deep reinforcement learning and demonstrations. In *Robotics: Science and Systems*, 2018.
- Stefan Schaal. Learning from demonstration. *Advances in neural information processing systems*, 9, 1996.
- Noah Y Siegel, Jost Tobias Springenberg, Felix Berkenkamp, Abbas Abdolmaleki, Michael Neunert, Thomas Lampe, Roland Hafner, and Martin Riedmiller. Keep doing what worked: Behavioral modelling priors for offline reinforcement learning. *arXiv preprint arXiv:2002.08396*, 2020.
- David Silver, Aja Huang, Chris J Maddison, Arthur Guez, Laurent Sifre, George Van Den Driessche, Julian Schrittwieser, Ioannis Antonoglou, Veda Panneershelvam, Marc Lanctot, et al. Mastering the game of go with deep neural networks and tree search. *nature*, 529(7587):484–489, 2016.
- Avi Singh, Albert Yu, Jonathan Yang, Jesse Zhang, Aviral Kumar, and Sergey Levine. Cog: Connecting new skills to past experience with offline reinforcement learning. *arXiv preprint arXiv:2010.14500*, 2020.
- Yuda Song, Yifei Zhou, Ayush Sekhari, Drew Bagnell, Akshay Krishnamurthy, and Wen Sun. Hybrid RL: Using both offline and online data can make RL efficient. In *The Eleventh International Conference on Learning Representations*, 2023. URL <https://openreview.net/forum?id=yyBis80iUuU>.
- Mel Vecerik, Todd Hester, Jonathan Scholz, Fumin Wang, Olivier Pietquin, Bilal Piot, Nicolas Heess, Thomas Rothörl, Thomas Lampe, and Martin Riedmiller. Leveraging demonstrations for deep reinforcement learning on robotics problems with sparse rewards. *arXiv preprint arXiv:1707.08817*, 2017.

- Oriol Vinyals, Igor Babuschkin, Wojciech M Czarnecki, Michaël Mathieu, Andrew Dudzik, Junyoung Chung, David H Choi, Richard Powell, Timo Ewalds, Petko Georgiev, et al. Grandmaster level in starcraft ii using multi-agent reinforcement learning. *Nature*, 575(7782):350–354, 2019.
- Andrew Wagenmaker and Aldo Pacchiano. Leveraging offline data in online reinforcement learning. *arXiv preprint arXiv:2211.04974*, 2022.
- Jialong Wu, Haixu Wu, Zihan Qiu, Jianmin Wang, and Mingsheng Long. Supported policy optimization for offline reinforcement learning. *arXiv preprint arXiv:2202.06239*, 2022.
- Chenjun Xiao, Han Wang, Yangchen Pan, Adam White, and Martha White. The in-sample softmax for offline reinforcement learning. In *International Conference on Learning Representations*, 2023. URL <https://openreview.net/forum?id=u-RuvyDYqCM>.
- Tengyang Xie and Nan Jiang. Q^* approximation schemes for batch reinforcement learning: A theoretical comparison. In *Conference on Uncertainty in Artificial Intelligence*, pages 550–559. PMLR, 2020.
- Tengyang Xie, Nan Jiang, Huan Wang, Caiming Xiong, and Yu Bai. Policy finetuning: Bridging sample-efficient offline and online reinforcement learning. *Advances in neural information processing systems*, 34:27395–27407, 2021.
- Deheng Ye, Guibin Chen, Wen Zhang, Sheng Chen, Bo Yuan, Bo Liu, Jia Chen, Zhao Liu, Fuhao Qiu, Hongsheng Yu, Yinyuting Yin, Bei Shi, Liang Wang, Tengfei Shi, Qiang Fu, Wei Yang, Lanxiao Huang, and Wei Liu. Towards playing full moba games with deep reinforcement learning. In H. Larochelle, M. Ranzato, R. Hadsell, M. F. Balcan, and H. Lin, editors, *Advances in Neural Information Processing Systems*, volume 33, pages 621–632. Curran Associates, Inc., 2020. URL <https://proceedings.neurips.cc/paper/2020/file/06d5ae105ea1bea4d800bc96491876e9-Paper.pdf>.
- Tianhe Yu, Garrett Thomas, Lantao Yu, Stefano Ermon, James Zou, Sergey Levine, Chelsea Finn, and Tengyu Ma. Mopo: Model-based offline policy optimization. *arXiv preprint arXiv:2005.13239*, 2020.
- Andrea Zanette, Martin J Wainwright, and Emma Brunskill. Provable benefits of actor-critic methods for offline reinforcement learning. *Advances in neural information processing systems*, 34:13626–13640, 2021.
- Yuexiang Zhai, Christina Baek, Zhengyuan Zhou, Jiantao Jiao, and Yi Ma. Computational benefits of intermediate rewards for goal-reaching policy learning. *Journal of Artificial Intelligence Research*, 73:847–896, 2022.
- Henry Zhu, Abhishek Gupta, Aravind Rajeswaran, Sergey Levine, and Vikash Kumar. Dexterous manipulation with deep reinforcement learning: Efficient, general, and low-cost. In *2019 International Conference on Robotics and Automation (ICRA)*, pages 3651–3657. IEEE, 2019.
- Yuke Zhu, Ziyu Wang, Josh Merel, Andrei Rusu, Tom Erez, Serkan Cabi, Saran Tunyasuvunakool, János Kramár, Raia Hadsell, Nando de Freitas, et al. Reinforcement and imitation learning for diverse visuomotor skills. *arXiv preprint arXiv:1802.09564*, 2018.

A. Implementation details of Cal-QL

Our algorithm, Cal-QL is illustrated in Algorithm 1. A complete implementation of the functions in python-style is provided in Appendix A.2.

A.1. Cal-QL Algorithm

We use $J_Q(\theta)$ to denote the calibrated conservative regularizer for the Q network update:

$$J_Q(\theta) := \alpha \underbrace{\left(\mathbb{E}_{s \sim \mathcal{D}, a \sim \pi} \left[\max \left(Q_\theta(s, a), Q^\mu(s, a) \right) \right] - \mathbb{E}_{s, a \sim \mathcal{D}} \left[Q_\theta(s, a) \right] \right)}_{\text{Calibrated conservative regularizer } \mathcal{R}(\theta)} + \frac{1}{2} \mathbb{E}_{s, a, s' \sim \mathcal{D}} \left[\left(Q_\theta(s, a) - \mathcal{B}^\pi \bar{Q}(s, a) \right)^2 \right]. \quad (\text{A.1})$$

Algorithm 1 Cal-QL pseudo-code

- 1: Initialize Q-function, Q_θ , a policy, π_ϕ
- 2: **for** step t in $\{1, \dots, N\}$ **do**
- 3: Train the Q-function using the conservative regularizer in Eq. A.1:

$$\theta_t := \theta_{t-1} - \eta_Q \nabla_\theta J_Q(\theta) \quad (\text{A.2})$$

- 4: Improve policy π_ϕ with SAC-style update:

$$\phi_t := \phi_{t-1} + \eta_\pi \mathbb{E}_{s \sim \mathcal{D}, a \sim \pi_\phi(\cdot|s)} \left[Q_\theta(s, a) - \log \pi_\phi(a|s) \right] \quad (\text{A.3})$$

- 5: If the online phase begins, change CQL regularizer coefficient α from α_{offline} to α_{online} .
 - 6: **end for**
-

A.2. Python Implementation

Listing 1: Training Q networks given a batch of data

```

cql_alpha = self.online_alpha if training_phase == 'online' else self.offline_alpha
q_data = critic(batch['observations'], batch['actions'])

next_dist = actor(batch['next_observations'])
next_pi_actions, next_log_pis = next_dist.sample()

target_qval = target_critic(batch['observations'], next_pi_actions)
target_qval = batch['rewards'] + self.gamma * (1 - batch['dones']) * target_qval

td_loss = mse_loss(q_data, target_qval)

num_samples = 4
random_actions = uniform((num_samples, batch_size, action_dim), min=-1, max=1)
random_pi = 0.5 ** batch['actions'].shape[-1]

pi_actions, log_pis = actor(batch['observations'])

q_rand_is = critic(batch['observations'], random_actions) - random_pi
q_pi_is = critic(batch['observations'], pi_actions) - log_pis

mc_return = batch['mc_return'].repeat(num_samples)
q_rand_is = max(q_rand_is, mc_return)
q_pi_is = max(q_pi_is, mc_return)

cat_q = concatenate([q_rand_is, q_pi_is], new_axis=True)
cat_q = logsumexp(cat_q, axis=0) # sum over num_samples
critic_loss = td_loss + ((cat_q - q_data).mean() * cql_alpha)

critic_optimizer.zero_grad()
critic_loss.backward()
critic_optimizer.step()

```

Listing 2: Training the policy (or the actor) given a batch of data

```

# return distribution of actions
pi_actions, log_pis = actor(batch['observations'])

# calculate q value of actor actions
qpi = critic(batch['observations'], actions)
qpi = qpi.min(axis=0)

# same objective as CQL (kumar et al.)
actor_loss = (log_pis * self.alpha - qpi).mean()

# optimize loss
actor_optimizer.zero_grad()
actor_loss.backward()
actor_optimizer.step()
    
```

B. Regret Analysis of Cal-QL

We provide a theoretical version of Cal-QL in Algorithm 2. Policy fine-tuning has been studied in different settings (Xie et al., 2021; Song et al., 2023; Wagenmaker and Pacchiano, 2022). Our analysis largely adopts the settings and results in Song et al. (2023), with additional changes in Assumption B.1, Assumption B.2, and Definition B.3. Note that the goal of this proof is to demonstrate that a *pessimistic functional class* (Assumption B.1) allows one to utilize the offline data efficiently, rather than providing a new analytical technique for regret analysis. See comparisons between Section B.3 and Section G.1. Note that we use f instead of Q_θ in the main text to denote the estimated Q function for notation simplicity.

Algorithm 2 Theoretical version of Cal-QL

- 1: **Input:** Value function class \mathcal{F} , # total iterations K , offline dataset \mathcal{D}_h^y of size m_{off} for $h \in [H - 1]$.
- 2: Initialize $f_h^1(s, a) = 0, \forall (s, a)$.
- 3: **for** $t = 1, \dots, K$ **do**
- 4: Let π^t be the greedy policy w.r.t. f^k ▷ I.e., $\pi_h^k(s) = \arg \max_a f_h^k(s, a)$.
- 5: For each h , collect m_{on} online tuples $\mathcal{D}_h^k \sim d_h^{\pi^k}$ ▷ online data collection
- 6: Set $f_H^{k+1}(s, a) = 0, \forall (s, a)$.
- 7: **for** $h = H - 1, \dots, 0$ **do** ▷ FQI with offline and online data
- 8: Estimate f_h^{k+1} using **conservative** least squares on the aggregated data: ▷ I.e., **CQL regularized class \mathcal{C}_h**

$$f_h^{k+1} \leftarrow \arg \min_{f \in \mathcal{C}_h} \left\{ \widehat{\mathbb{E}}_{\mathcal{D}_h^y} \left[f(s, a) - r - \max_{a'} f_{h+1}^{k+1}(s', a') \right]^2 + \sum_{\tau=1}^k \widehat{\mathbb{E}}_{\mathcal{D}_h^\tau} \left[f(s, a) - r - \max_{a'} f_{h+1}^{k+1}(s', a') \right]^2 \right\} \quad (\text{B.1})$$

- 9: $f_h^{k+1} = \max\{f_h^{k+1}, Q_h^{\text{ref}}\}$ ▷ Set the return of a reference policy as lower bound
- 10: **end for**
- 11: **end for**
- 12: **Output:** π^K

B.1. Preliminaries

In this subsection, we follow most of the notations and definitions in Song et al. (2023). In particular, we consider the finite horizon cases, where the value function and Q function are defined as:

$$V_h^\pi(s) = \mathbb{E} \left[\sum_{\tau=h}^{H-1} r_\tau | \pi, s_h = s \right] \quad (\text{B.2})$$

$$Q_h^\pi(s, a) = \mathbb{E} \left[\sum_{\tau=h}^{H-1} r_\tau | \pi, s_h = s, a_h = a \right]. \quad (\text{B.3})$$

We also define the Bellman operator \mathcal{T} such that $\forall f : \mathcal{S} \times \mathcal{A}$:

$$\mathcal{T}f(s, a) = \mathbb{E}_{s,a}[R(s, a)] + \mathbb{E}_{s' \sim P(s,a)} \max_{a'} f(s', a'), \quad \forall (s, a) \in \mathcal{S} \times \mathcal{A}, \quad (\text{B.4})$$

where $R(s, a) \in \Delta[0, 1]$ represents a stochastic reward function.

B.2. Notations

- Feature covariance matrix $\Sigma_{k;h}$:

$$\Sigma_{k;h} = \sum_{\tau=1}^k X_h(f^\tau)(X_h(f^\tau))^\top + \lambda \mathbf{I} \quad (\text{B.5})$$

- Matrix Norm [Zanette et al. \(2021\)](#): for a matrix Σ , the matrix norm $\|\mathbf{u}\|_\Sigma$ is defined as:

$$\|\mathbf{u}\|_\Sigma = \sqrt{\mathbf{u}\Sigma\mathbf{u}^\top} \quad (\text{B.6})$$

- Weighted ℓ^2 norm: for a given distribution $\beta \in \Delta(\mathcal{S} \times \mathcal{A})$ and a function $f : \mathcal{S} \times \mathcal{A} \mapsto \mathbb{R}$, we denote the weighted ℓ^2 norm as:

$$\|f\|_{2,\beta}^2 := \sqrt{\mathbb{E}_{(s,a) \sim \beta} f^2(s,a)} \quad (\text{B.7})$$

- A stochastic reward function $R(s,a) \in \Delta([0,1])$
- For each offline data distribution $\nu = \{\nu_0, \dots, \nu_{H-1}\}$, the offline data set at time step h (ν_h) contains data samples (s,a,r,s') , where $(s,a) \sim \nu_h$, $r \in R(s,a)$, $s' \sim P(s,a)$.
- Given a policy $\pi := \{\pi_0, \dots, \pi_{H-1}\}$, where $\pi_h : \mathcal{S} \mapsto \Delta(\mathcal{A})$, $d_h^\pi \in \Delta(\mathcal{S}, \mathcal{A})$ denotes the state-action occupancy induced by π at step h .
- We consider the value-based function approximation setting, where we are given a function class $\mathcal{C} = \mathcal{C}_0 \times \dots \times \mathcal{C}_{H-1}$ with $\mathcal{C}_h \subset \mathcal{S} \times \mathcal{A} \mapsto [0, V_{\max}]$.
- A policy π^f is defined as the greedy policy w.r.t. f : $\pi_h^f(s) = \arg \max_a f_h(s,a)$. Specifically, at iteration k , we use π^k to denote the greedy policy w.r.t. f^k .

B.3. Assumptions and Defintions

Assumption B.1 (Pessimistic Realizability and Completeness). For any policy π^e , we say \mathcal{C}_h is a pessimistic function class w.r.t. π^e , if for any h , we have $Q_h^{\pi^e} \in \mathcal{C}_h$, and additionally, for any $f_{h+1} \in \mathcal{C}_{h+1}$, we have $\mathcal{T}f_{h+1} \in \mathcal{C}_h$ and $f_h(s,a) \leq Q_h^{\pi^e}(s,a), \forall (s,a) \in \mathcal{S} \times \mathcal{A}$.

Assumption B.2 (Bilinear Rank of Reference Policies). Suppose $Q^{\text{ref}} \in \mathcal{C}_{\text{ref}} \subset \mathcal{C}$, where \mathcal{C}_{ref} is the function class of our reference policy, we assume the Bilinear rank of \mathcal{C}_{ref} is d_{ref} and $d_{\text{ref}} \leq d$.

Definition B.3 (Bellman error transfer coefficient). For any policy π , we define the transfer coefficient on \mathcal{C} as

$$C_\pi := \max_{f \in \mathcal{C}} \frac{\sum_{h=0}^{H-1} \mathbb{E}_{s,a \sim d_h^\pi} [\mathcal{T}f_{h+1}(s,a) - f_h(s,a)]}{\sqrt{\sum_{h=0}^{H-1} \mathbb{E}_{s,a \sim \nu_h} (\mathcal{T}f_{h+1}(s,a) - f_h(s,a))^2}} \quad (\text{B.8})$$

Definition B.4 (Calibrated Bellman error transfer coefficient). For any policy π , we define the calibrated transfer coefficient w.r.t. to a reference policy π^{ref} as

$$C_\pi^{\text{ref}} := \max_{f \in \mathcal{C}, f(s,a) \geq Q^{\text{ref}}(s,a)} \frac{\sum_{h=0}^{H-1} \mathbb{E}_{s,a \sim d_h^\pi} [\mathcal{T}f_{h+1}(s,a) - f_h(s,a)]}{\sqrt{\sum_{h=0}^{H-1} \mathbb{E}_{s,a \sim \nu_h} (\mathcal{T}f_{h+1}(s,a) - f_h(s,a))^2}} \quad (\text{B.9})$$

where $Q^{\text{ref}} = Q^{\pi^{\text{ref}}}$.

By the definition of C_π^{ref} and C_π , we naturally have $C_\pi^{\text{ref}} \leq C_\pi$.

B.4. Our Results

Theorem B.5 (Formal Result of Theorem 6.1). Fix $\delta \in (0,1)$, $m_{\text{off}} = K$, $m_{\text{on}} = 1$, suppose and the function class \mathcal{C} follows Assumption B.1 w.r.t. π^e . Suppose the underlying MDP admits Bilinear rank d on function class \mathcal{C} and d_{ref} on \mathcal{C}_{ref} , respectively, then with probability at least $1 - \delta$, Algorithm 2 obtains the following bound on cumulative suboptimality w.r.t. any comparator policy π^e :

$$\sum_{t=1}^K V^{\pi^e} - V^{\pi^k} = \tilde{O} \left(\min \left\{ C_{\pi^e}^{\text{ref}} H \sqrt{dK \log(|\mathcal{F}|/\delta)}, K \left(V^{\pi^e} - V^{\text{ref}} \right) + H \sqrt{d_{\text{ref}} K \log(|\mathcal{F}|/\delta)} \right\} \right). \quad (\text{B.10})$$

Note that Theorem B.5 provides a guarantee for *any* comparator policy π^e , which can be directly applied to π^* described in our informal result (Theorem 6.1). We also change the notation for the reference policy from μ in Theorem 6.1 to π^{ref} (similarly, $d_{\text{ref}}, V^{\text{ref}}, C_{\pi^e}^{\text{ref}}$ correspond to $d_\mu, V^\mu, C_{\pi^e}^\mu$ in Theorem 6.1) for notation consistency in the proof. Our proof of Theorem B.5 largely follows the proof of Theorem 1 of (Song et al., 2023), and the major changes are caused by Assumption B.1, Assumption B.2, Definition B.3, and Definition B.4.

Proof. Let $V^{\text{ref}}(s) = \max_a Q^{\text{ref}}(s, a)$, we start by noting that

$$\begin{aligned}
 \sum_{k=1}^K V^{\pi^e} - V^{\pi^{fk}} &= \sum_{k=1}^K \mathbb{E}_{s \sim \rho} \left[V_0^{\pi^e}(s) - V_0^{\pi^{fk}}(s) \right] \\
 &= \underbrace{\sum_{k=1}^K \mathbb{E}_{s \sim \rho} \left[\mathbb{1} \{ \bar{\mathcal{E}}_k \} \left(V_0^{\pi^e}(s) - V^{\text{ref}}(s) \right) \right]}_{\Gamma_0} + \underbrace{\sum_{k=1}^K \mathbb{E}_{s \sim \rho} \left[\mathbb{1} \{ \bar{\mathcal{E}}_k \} \left(V^{\text{ref}}(s) - \max_a f_0^k(s, a) \right) \right]}_{=0, \text{ by the definition of } \bar{\mathcal{E}}_k} \\
 &\quad + \underbrace{\sum_{t=1}^K \mathbb{E}_{s \sim \rho} \left[\mathbb{1} \{ \bar{\mathcal{E}}_k \} \left(\max_a f_0^k(s, a) - V_0^{\pi^{fk}}(s) \right) \right]}_{\Gamma_1} + \underbrace{\sum_{k=1}^K \mathbb{E}_{s \sim \rho} \left[\mathbb{1} \{ \mathcal{E}_k \} \left(V_0^{\pi^e}(s) - \max_a f_0^k(s, a) \right) \right]}_{\Gamma_2} \\
 &\quad + \underbrace{\sum_{t=1}^T \mathbb{E}_{s \sim \rho} \left[\mathbb{1} \{ \mathcal{E}_k \} \left(\max_a f_0^k(s, a) - V_0^{\pi^{fk}}(s) \right) \right]}_{\Gamma_3}.
 \end{aligned} \tag{B.11}$$

Let $K_1 = \sum_{k=1}^K \mathbb{1} \{ f_0^k(s, a) > Q^{\text{ref}}(s, a) \}$ and $K_2 = \sum_{k=1}^K \mathbb{1} \{ f_0^k(s, a) \leq Q^{\text{ref}}(s, a) \}$. For Γ_0 , we have

$$\Gamma_0 = K_2 \mathbb{E}_{s \sim \rho} \left(V^{\pi^e}(s) - V^{\text{ref}}(s) \right). \tag{B.12}$$

For Γ_2 , we have

$$\begin{aligned}
 \Gamma_2 &= \sum_{k=1}^K \mathbb{E}_{s \sim \rho} \left[\mathbb{1} \{ \mathcal{E}_k \} \left(V_0^{\pi^e}(s) - \max_a f_0^k(s, a) \right) \right] \stackrel{(i)}{\leq} \sum_{k=1}^K \mathbb{1} \{ \mathcal{E}_k \} \sum_{h=0}^{H-1} \mathbb{E}_{s, a \sim d_h^{\pi^e}} \left[\mathcal{T} f_{h+1}^k(s, a) - f_h^k(s, a) \right] \\
 &\stackrel{(ii)}{\leq} \sum_{k=1}^K \left[C_{\pi^e}^{\text{ref}} \cdot \mathbb{1} \{ \mathcal{E}_k \} \sqrt{\sum_{h=0}^{H-1} \mathbb{E}_{s, a \sim \nu_h} \left[\left(f_h^k(s, a) - \mathcal{T} f_{h+1}^k(s, a) \right)^2 \right]} \right] \stackrel{(iii)}{\leq} K_1 C_{\pi^e}^{\text{ref}} \sqrt{H \cdot \Delta_{\text{off}}},
 \end{aligned} \tag{B.13}$$

where inequality (i) holds because of Lemma G.6, inequality (ii) holds by the definition of $C_{\pi^e}^{\text{ref}}$ (Definition B.4), inequality (iii) holds by Lemma G.5, and Assumption B.3. Note that the telescoping decomposition technique in the above equation also appears in (Xie and Jiang, 2020; Jin et al., 2021a; Du et al., 2021). Next, we will bound $\Gamma_1 + \Gamma_3$:

$$\begin{aligned}
 \Gamma_1 + \Gamma_3 &= \sum_{k=1}^K \left(\mathbb{1} \{ \mathcal{E}_k \} + \mathbb{1} \{ \bar{\mathcal{E}}_k \} \right) \mathbb{E}_{s \sim d_0} \left[\max_a f_0^k(s, a) - V_0^{\pi^{fk}}(s) \right] \\
 &\stackrel{(i)}{\leq} \sum_{k=1}^K \left(\mathbb{1} \{ \mathcal{E}_k \} + \mathbb{1} \{ \bar{\mathcal{E}}_k \} \right) \sum_{h=0}^{H-1} \left| \mathbb{E}_{s, a \sim d_h^{\pi^{fk}}} \left[f_h^k(s, a) - \mathcal{T} f_{h+1}^k(s, a) \right] \right| \\
 &\stackrel{(ii)}{=} \sum_{i=1}^K \left[\left(\mathbb{1} \{ \mathcal{E}_k \} + \mathbb{1} \{ \bar{\mathcal{E}}_k \} \right) \sum_{h=0}^{H-1} \left| \left\langle X_h(f^k), W_h(f^k) \right\rangle \right| \right] \\
 &\stackrel{(iii)}{\leq} \sum_{k=1}^K \left[\left(\mathbb{1} \{ \mathcal{E}_k \} + \mathbb{1} \{ \bar{\mathcal{E}}_k \} \right) \sum_{h=0}^{H-1} \|X_h(f^k)\|_{\Sigma_{k-1, h}^{-1}} \sqrt{\Delta_{\text{on}} + \lambda B_W^2} \right],
 \end{aligned} \tag{B.14}$$

where inequality (i) holds by Lemma G.7, equation (ii) holds by the definition of Bilinear model (equation G.1 in

Definition G.2), inequality (ii) holds by Lemma G.8. Using Lemma G.9, we have that

$$\begin{aligned}
 \Gamma_1 + \Gamma_3 &\leq \sum_{k=1}^K \left[\left(\mathbb{1}\{\mathcal{E}_k\} + \mathbb{1}\{\bar{\mathcal{E}}_k\} \right) \sum_{h=0}^{H-1} \left\| X_h(f^k) \right\|_{\Sigma_{k-1;h}^{-1}} \sqrt{\Delta_{\text{on}} + \lambda B_W^2} \right] \\
 &\stackrel{(i)}{\leq} H \sqrt{2d \log \left(1 + \frac{K_1 B_X^2}{\lambda d} \right) \cdot (\Delta_{\text{on}} + \lambda B_W^2) \cdot K_1} + H \sqrt{2d_{\text{ref}} \log \left(1 + \frac{K_2 B_X^2}{\lambda d_{\text{ref}}} \right) \cdot (\Delta_{\text{on}} + \lambda B_W^2) \cdot K_2} \\
 &\stackrel{(ii)}{\leq} H \left(\sqrt{2d \log \left(1 + \frac{K_1}{d} \right) \cdot (\Delta_{\text{on}} + B_X^2 B_W^2) \cdot K_1} + \sqrt{2d_{\text{ref}} \log \left(1 + \frac{K_2}{d_{\text{ref}}} \right) \cdot (\Delta_{\text{on}} + B_X^2 B_W^2) \cdot K_2} \right),
 \end{aligned} \tag{B.15}$$

where inequality (i) holds by the assumption that C_{ref} has bilinear rank d_{ref} , and inequality (ii) holds by plugging in $\lambda = B_X^2$. Substituting equation B.12, inequality B.13, and inequality equation B.15 into equation B.11, we have

$$\begin{aligned}
 \sum_{i=1}^K V^{\pi^e} - V^{\pi^{f^k}} &\leq \Gamma_0 + \Gamma_2 + \Gamma_1 + \Gamma_3 \leq K_2 \left(V^{\pi^e}(s) - V^{\text{ref}}(s) \right) + K_1 C_{\pi^e}^{\text{ref}} \sqrt{H \cdot \Delta_{\text{off}}} \\
 &+ H \left(\sqrt{2d \log \left(1 + \frac{K_1}{d} \right) \cdot (\Delta_{\text{on}} + B_X^2 B_W^2) \cdot K_1} + \sqrt{2d_{\text{ref}} \log \left(1 + \frac{K_2}{d_{\text{ref}}} \right) \cdot (\Delta_{\text{on}} + B_X^2 B_W^2) \cdot K_2} \right)
 \end{aligned} \tag{B.16}$$

Plugging in the values of $\Delta_{\text{on}}, \Delta_{\text{off}}$ from equation G.4 and equation G.5, and using the subadditivity of the square root function, we have

$$\begin{aligned}
 \sum_{k=1}^K V^{\pi^e} - V^{\pi^{f^k}} &\leq K_2 \left(V^{\pi^e}(s) - V^{\text{ref}}(s) \right) + 16V_{\text{max}} C_{\pi^e}^{\text{ref}} K_1 \sqrt{\frac{H}{m_{\text{off}}} \log \left(\frac{2HK_1|\mathcal{F}|}{\delta} \right)} \\
 &+ \left(16V_{\text{max}} \sqrt{\frac{1}{m_{\text{on}}} \log \left(\frac{2HK_1|\mathcal{F}|}{\delta} \right)} + B_X B_W \right) \cdot H \sqrt{2dK_1 \log \left(1 + \frac{K_1}{d} \right)} \\
 &+ \left(16V_{\text{max}} \sqrt{\frac{1}{m_{\text{on}}} \log \left(\frac{2HK_2|\mathcal{F}|}{\delta} \right)} + B_X B_W \right) \cdot H \sqrt{2d_{\text{ref}}K_2 \log \left(1 + \frac{K_2}{d_{\text{ref}}} \right)}
 \end{aligned} \tag{B.17}$$

Setting $m_{\text{off}} = K, m_{\text{on}} = 1$ in the above equation completes the proof, we have

$$\begin{aligned}
 \sum_{k=1}^K V^{\pi^e} - V^{\pi^k} &\leq \tilde{O} \left(C_{\pi^e}^{\text{ref}} \sqrt{HK_1 \log(|\mathcal{F}|/\delta)} \right) + \tilde{O} \left(H \sqrt{dK_1 \log(|\mathcal{F}|/\delta)} \right) \\
 &+ K_2 \left(V^{\pi^e}(s) - V^{\text{ref}}(s) \right) + \tilde{O} \left(H \sqrt{d_{\text{ref}}K_2 \log(|\mathcal{F}|/\delta)} \right) \\
 &\leq \begin{cases} \tilde{O} \left(C_{\pi^e}^{\text{ref}} H \sqrt{dK_1 \log(|\mathcal{F}|/\delta)} \right) & \text{if } K_1 \gg K_2, \\ \tilde{O} \left(K_2 \left(V^{\pi^e} - V^{\text{ref}} \right) + H \sqrt{d_{\text{ref}}K_2 \log(|\mathcal{F}|/\delta)} \right) & \text{otherwise.} \end{cases} \\
 &\leq \tilde{O} \left(\min \left\{ C_{\pi^e}^{\text{ref}} H \sqrt{dK \log(|\mathcal{F}|/\delta)}, K \left(V^{\pi^e} - V^{\text{ref}} \right) + H \sqrt{d_{\text{ref}}K \log(|\mathcal{F}|/\delta)} \right\} \right),
 \end{aligned} \tag{B.18}$$

where the last inequality holds because $K_1, K_2 \leq K$, which completes the proof. \square

C. Environment Details

C.1. Antmaze

The antmaze navigation tasks aim to control an 8-DoF ant quadruped robot to move from a starting point to a desired goal in a maze. The agent will receive sparse +1/0 rewards depending on whether it reaches the goal or not. We study each method on “medium” and “hard” (shown in Figure 5) mazes which are difficult to solve, using the following datasets from D4RL (Fu et al., 2020): large-diverse, large-play, medium-diverse, and medium-play. The difference between “diverse” and “play” datasets is the optimality of the trajectories they contain. The “diverse” datasets contain the trajectories commanded to a random goal from random starting points, while the “play” datasets contain the trajectories commanded to specific locations which are not necessarily the goal. For Cal-QL CQL and IQL, we pre-trained the agent using the offline dataset for 1M steps.

C.2. Franka Kitchen

The `kitchen` tasks require controlling a 9-DoF Franka robot to arrange a kitchen environment into a desired configuration. The configuration is decomposed into 4 subtasks, and the agent will receive rewards of 0, +1, +2, +3, or +4 depending on how many subtasks it has managed to solve. To solve the whole task and reach the desired configuration, it is important to learn not only how to solve each subtask, but also to figure out the correct order to solve. We study this domain using datasets with three different optimalities: `kitchen-complete`, `kitchen-partial`, and `kitchen-mixed`. The “complete” dataset contains the trajectories of the robot performing the whole task completely. The “partial” dataset partially contains some complete demonstrations, while others are incomplete demonstrations solving the subtasks. The “mixed” dataset only contains incomplete data without any complete demonstrations, which is hard and requires the highest degree of stitching and generalization ability. For Cal-QL, CQL, and IQL, we pre-trained the agent using the offline dataset for 500K steps.

C.3. Adroit

The Adroit domain involves controlling a 24-DoF shadow hand robot. There are 3 tasks we consider in this domain: `pen-binary`, `relocate-binary`, `relocate-binary`. These tasks comprise a limited set of narrow human expert data distributions (~ 25) with additional trajectories collected by a behavior-cloned policy. We truncated each trajectory and used the positive segments (terminate when the positive reward signal is found) for all methods. This domain has a very narrow dataset distribution and a large action space. In addition, learning in this domain is difficult due to the sparse reward formulation, which leads to exploration challenges. We utilized a variant of the dataset used in prior work (Nair et al., 2020a) to have a standard comparison with SOTA offline fine-tuning experiments that consider this domain. For the offline learning phase, we pre-trained the agent for 20K steps.

C.4. Visual Manipulation Domain

The Visual Manipulation domain consists of a pick-and-place task. This task is a multitask formulation explored in the work, Pre-training for Robots (PTR) (Kumar et al., 2022). Here each task is defined as placing an object in a bin. A distractor object was present in the scene as an adversarial object which the agent had to avoid picking. There were 10 unique objects and no overlap between the task objects and the interfering/distractor objects. For the offline phase, we pre-trained the policy with offline data for 50K steps.

D. Experiment Details

D.1. Normalized Scores for all Tasks

The `visual-manipulation`, `adroit`, and `antmaze` domains are all goal-oriented, sparse reward tasks. In these domains, we computed the normalized metric as simply the goal achieved rate for each method. For example, in the visual manipulation environment, if the object was placed successfully in the bin, a +1 reward was given to the agent and the task is completed. Similarly, for the `door-binary` task in the adroit tasks, we considered the success rate of opening the door.

For the `kitchen` task, the task is to solve a series of 4 sub-tasks that need to be solved in an iterative manner. The normalized score is computed simply as $\frac{\text{\#tasks solved}}{\text{total tasks}}$.

D.2. Mixing Ratio Hyperparameter

In this work, we explore the mixing ratio parameter m , which is used during the online fine-tuning phase. The mixing ratio is either a value in the range $[0, 1]$ or the value -1. If this mixing ratio is within $[0, 1]$, it represents what percentage of offline and online data is seen in each batch when fine-tuning. For example, if the mixing ratio $m = 0.25$, that means for each batch we sample 25% from the offline data and 75% from online data. Instead, if the mixing ratio is -1, the buffers are appended to each other and sampled uniformly.

D.3. Hyperparameters for CQL and Cal-QL

Here we list the hyperparameters for CQL and Cal-QL in Table 3. For each domain, we ablated over the values of offline α , online α , and mixing ratio. The values highlighted in bold represent the final selection. We utilized a variant of Bellman backup that computes the target value by performing a maximization over target values computed for k actions sampled from the policy at the next state, where we used $k = 4$ in visual pick and place domain and $k = 10$ in others. In the Antmaze domain, we used the dual version of CQL (Kumar et al., 2020) and conducted ablations over the value of the threshold of the CQL regularizer $\mathcal{R}(\theta)$ (target action gap) instead of offline and online α .

D.4. Hyperparameters for IQL

Here we list the hyperparameters for IQL in Table 4. To conduct our experiments, we used the official implementation of IQL provided by the authors and primarily followed their recommended parameters, which they previously ablated over in their work. Below, we present the chosen parameters as well as the additional parameters we swept over.

D.5. Hyperparameters for SAC, SAC + Offline Data

We use the standard hyperparameters for SAC as derived from the original implementation in (Haarnoja et al., 2018a). We used the same other hyperparameters as CQL and Cal-QL. We used automatic entropy tuning for the policy and critic entropy terms, with a target entropy of the negative action dimension.

Table 3: CQL, Cal-QL Hyperparameters

Hyperparameters	Adroit	Kitchen	Antmaze	Manipulation
offline α	0.1, 1 , 5, 10, 20	1, 5	-	1, 5 , 10
online α	0.1, 1 , 5, 10, 20	1, 5	-	0, 0.5 , 1, 5
target action gap	-	-	0.1, 0.4, 0.8	-
mixing ratio	-1, 0.25, 0.5	-1, 0.25 , 0.5	0.5	0.2, 0.5 , 0.7, 0.9
policy architecture	512-512	512-512-512	256-256	ConvNet
policy learning rate	1e-4	1e-4	1e-4	1e-4
critic architecture	512-512-512	512-512-512	256-256-256-256	ConvNet
critic learning rate	3e-4	3e-4	3e-4	3e-4
reward scale	10	1	10	11
reward bias	5	1	-5	-1
pre-training steps	20K	500K	1M	50K
batch size	256	256	256	64

Table 4: IQL Hyperparameters

Hyperparameters	Adroit	Kitchen	Antmaze	Manipulation
expectile τ	0.8	0.7	0.9	0.5, 0.6, 0.7 , 0.8, 0.9, 0.95, 0.99
temperature β	3	0.5	10	1, 3, 5, 10 , 25, 50
mixing ratio	0.2 , 0.5	-1, 0.25 , 0.5	0.5	0.2, 0.5 , 0.7, 0.9
policy architecture	256-256	256-256	256-256	ConvNet
policy learning rate	3e-4	3e-4	3e-4	1e-4
critic architecture	256-256	256-256	256-256	ConvNet
critic learning rate	3e-4	3e-4	3e-4	3e-4
pre-training steps	20K	500K	1M	50K
batch size	256	256	256	64

E. Extended Discussion on Limitations of Existing Fine-Tuning Methods

In this section, we aim to highlight some potential reasons behind the slow improvement of IQL in our empirical analysis experiment in Section 4.1. We first swept over the temperature β values for IQL, which controls the constraint on how closely the learned policy should match the behavior policy. As shown in Figure 11, the change in the temperature β has little to no effect on the sample efficiency. Another natural hypothesis is that IQL improves slowly because we are not making enough updates per unit of data collected by the environment. To investigate this, we ran IQL with (a) five times as many gradient steps per step of data collection (UTD = 5), and (b) with a more aggressive policy update. Observe in Figure 12 that (a) does not improve the asymptotic performance of IQL, although it does

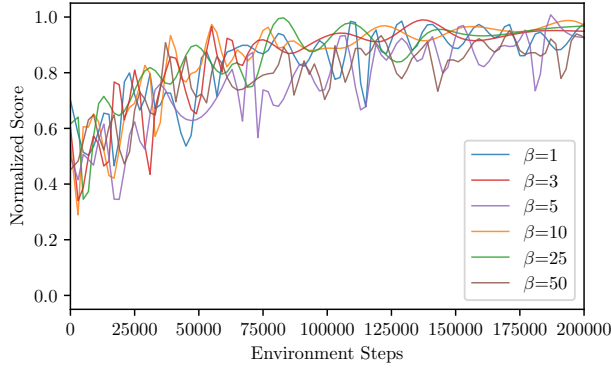


Figure 11: IQL Ablation: We show how the change in the temperature β has little to no effect on the sample efficiency.

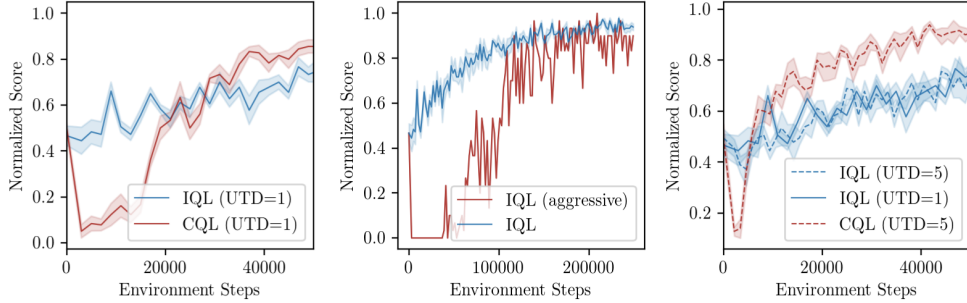


Figure 12: IQL and CQL: Step 0 on the x-axis is the performance after offline pre-training. Observe while CQL suffers from initial policy unlearning, IQL improves slower throughout fine-tuning.

improve CQL meaning that there is room for improvement on this task by making more gradient updates. Observe in Figure 12 that (b) often induces policy unlearning, similar to the failure mode in CQL. These two observations together indicate that a policy constraint approach can slow down learning asymptotically, and we cannot increase the speed by making more aggressive updates as this causes the policy to find erroneously optimistic out-of-distribution actions, and unlearn the policy learned from offline data. An alternative would be for our method to altogether avoid policy constraints.

F. Discussion of Policy Unlearning in Fine-Tuning

F.1. Bellman Consistency Equation of CQL

To analyze policy unlearning with conservative methods at the beginning of online fine-tuning, we consider a tabular setting, where we are learning conservative value functions using a generic policy-iteration style offline RL method based on CQL (Kumar et al., 2020). Our goal is to understand the differences in a policy obtained by running one round of policy improvement with and without additional online data. Key to our analysis is the Bellman backup induced by CQL (Equation 3.1):

$$Q^\pi(s, a) = (\mathcal{B}^\pi Q^\pi)(s, a) - \alpha \left[\frac{\pi(a|s)}{\pi_\beta(a|s)} - 1 \right]. \quad (\text{F.1})$$

By expanding \mathcal{B}^π , Equation F.1 can also be interpreted as running standard Q-iteration in an MDP with a pessimistic reward function, which depends upon the learned policy π , the behavior policy π_β induced by the dataset, and the coefficient α from Equation 3.1: $r_{\alpha, \beta}^\pi(s, a) = r(s, a) - \alpha \left[\frac{\pi(a|s)}{\pi_\beta(a|s)} - 1 \right]$. This means that once online fine-tuning commences with a new regularizer α , and a new behavior policy $\pi_{\beta'}$ induced by online data added to the buffer, the pessimistic reward function $r_{\alpha, \beta}^\pi$ may bias towards $r_{\alpha', \beta'}^\pi$. Hence, the policy improvement on the resulting Q-function with the

online data may simply not lead to any policy improvement on the ground-truth reward function. We will first provide a condition such that the pessimistic Q-function is invariant to such reward bias during the online fine-tuning, and then show how our approach alleviates the reward bias.

Performance difference during fine-tuning. Consider the fixed points from solving Equation F.1 w.r.t. the biased rewards $r_{\alpha,\beta}^\pi$ and $r_{\alpha',\beta'}^\pi$. Theorem F.1 provides a necessary and sufficient condition for the fixed points to be invariant to reward bias.

Theorem F.1 (Invariant Conservative Q Functions). *Let Q and Q' denote the conservative value function from solving the fixed point Equation F.1 with regularizers α, α' and behavior policies $\pi_\beta, \pi_{\beta'}$ respectively. Then for a given policy π , $Q(s, a) = Q'(s, a), \forall s \in \mathcal{S}$ if and only if*

$$\frac{\alpha}{\pi_\beta(a|s)} - \frac{\alpha'}{\pi_{\beta'}(a|s)} = \frac{\alpha - \alpha'}{\pi(a|s)}, \quad \forall (s, a) \in \mathcal{S} \times \mathcal{A}. \quad (\text{F.2})$$

The proof of Theorem F.1 is provided in Appendix F.5. Theorem F.1 implies that one shall expect a performance change in the fine-tuning phase, whenever Equation F.2 becomes invalid. Unfortunately, Equation F.2 is generally hard to enforce in practice since the new behavior policy $\pi_{\beta'}$ and the updated policy π may be intractable, as suggested by the performance dip in Section 4.1.

Preventing unlearning via calibration. Since the standard CQL training objective suffers from reward bias, which may continue to deteriorate during fine-tuning. The next corollary provides a condition under which $r_{\alpha,\beta}^\pi(s, a)$ becomes unbiased.

Corollary F.2. *The reward function $r_{\alpha,\beta}^\pi(s, a)$ induced by the CQL training (Equation F.1) becomes unbiased when $\pi = \pi_\beta$: $r_{\alpha,\beta}^\pi(s, a) = r(s, a), \forall (s, a) \in \mathcal{S} \times \mathcal{A}$.*

The proof of Corollary F.2 is straight forward as substituting $\pi = \pi_\beta$ will set $\left[\frac{\pi(a|s)}{\pi_\beta(a|s)} - 1 \right] = 0$, which makes Equation F.1 become a Bellman backup w.r.t. the original reward $r(s, a)$. Corollary F.2 implies that the CQL-induced Bellman backup (Equation 3.1) becomes unbiased when the updating policy equals the behavior policy. Hence, if one aims at using a neural network Q_θ to approximate the CQL Bellman backup w.r.t. behavior policy π_β , one shall consider using $Q^{\pi_\beta}(s, a)$ to calibrate the bias. This empirically implies that we shall use $Q^{\pi_\beta}(s, a)$ and $Q^{\pi_{\beta'}}(s, a)$ to calibrate the Q_θ during offline and online phase, as we have presented in Definition 4.1 and Section 5.

F.2. Notations

In this subsection, we provide the notations for deriving the Bellman Consistency Equation of the conservative Bellman Consistency equation (CQL Objective) equation F.1. Our matrix notation follows (Li et al., 2020).

- We consider the infinite horizon tabular setting where \mathcal{S} and \mathcal{A} are discrete and finite, $\gamma \in (0, 1)$ is a discount factor and $r : \mathcal{S} \times \mathcal{A} \mapsto [0, 1]$ is the reward function;
- The value function $V^\pi(s)$ of a state w.r.t. policy π is defined as

$$V^\pi(s) := \mathbb{E} \left[\sum_{t=0}^{\infty} \gamma^t r(s^t, a^t) \mid s^0 = s \right], \quad \forall s \in \mathcal{S}; \quad (\text{F.3})$$

- The Q function $Q^\pi(s, a)$ of a state action pair (s, a) w.r.t. a policy π is defined by

$$Q^\pi(s, a) := \mathbb{E} \left[\sum_{t=0}^{\infty} \gamma^t r(s^t, a^t) \mid s^0 = s, a^0 = a \right] \quad \forall (s, a) \in \mathcal{S} \times \mathcal{A}; \quad (\text{F.4})$$

- $\mathbf{P} \in \mathbb{R}^{|\mathcal{S}| \times |\mathcal{A}| \times |\mathcal{S}|}$ is a matrix of the transition kernel P ;
- $\mathbf{P}^\pi \in \mathbb{R}^{|\mathcal{S}| \times |\mathcal{A}| \times |\mathcal{S}| \times |\mathcal{A}|}$ and $\mathbf{P}_\pi \in \mathbb{R}^{|\mathcal{S}| \times |\mathcal{S}|}$ two square probability transition matrices induced by the policy π over the state-action pair and the states respectively, defined by

$$\mathbf{P}^\pi := \mathbf{P}\mathbf{\Pi}^\pi, \quad \mathbf{P}_\pi := \mathbf{\Pi}^\pi \mathbf{P}; \quad (\text{F.5})$$

- $\mathbf{\Pi}^\pi \in \{0, 1\}^{|\mathcal{S}| \times |\mathcal{S}| \times |\mathcal{A}|}$ is a projection matrix:

$$\mathbf{\Pi}^\pi = \begin{pmatrix} \mathbf{e}_{\pi(1)}^\top & & & \\ & \mathbf{e}_{\pi(2)}^\top & & \\ & & \ddots & \\ & & & \mathbf{e}_{\pi(|\mathcal{S}|)}^\top \end{pmatrix} \quad (\text{F.6})$$

- $\mathbf{r} \in \mathbb{R}^{|\mathcal{S}| \times |\mathcal{A}|}$ is the reward function
- $\mathbf{r}^\pi \in \mathbb{R}^{|\mathcal{S}|}$ is the reward function following policy π , simply we have $\mathbf{r}^\pi = \mathbf{\Pi}^\pi \mathbf{r}$.

F.3. Derivations of Conservative Bellman Consistency Equation F.1

$\forall (s, a) \in \mathcal{S} \times \mathcal{A}$, the tabular CQL optimization (Equation 3.1) aims at solving the following optimization problem:

$$\min_{Q(s,a)} \alpha \left[\mathbb{E}_{s \sim \mathcal{D}, a \sim \pi} Q(s, a) - \mathbb{E}_{(s,a) \sim \mathcal{D}, a \sim \pi_\beta} Q(s, a) \right] + \frac{1}{2} \mathbb{E}_{s \sim \mathcal{D}, a \sim \pi_\beta} \left[(Q(s, a) - \mathcal{B}^\pi Q(s, a))^2 \right]. \quad (\text{F.7})$$

If we rewrite $x = Q(s, a)$ and define function $f(x)$ as

$$f(x) := \alpha \left[\mathbb{E}_{s \sim \mathcal{D}, a \sim \pi} x - \mathbb{E}_{(s,a) \sim \mathcal{D}, a \sim \pi_\beta} x \right] + \frac{1}{2} \mathbb{E}_{s \sim \mathcal{D}, a \sim \pi_\beta} \left[(x - \mathcal{B}^\pi x)^2 \right], \quad (\text{F.8})$$

setting $f'(x) = 0$ yields

$$\alpha (\pi(a|s) - \pi_\beta(a|s)) + \pi_\beta(x - \mathcal{B}^\pi x) = 0, \quad (\text{F.9})$$

which leads to

$$x = \mathcal{B}^\pi x - \alpha \left[\frac{\pi(a|s)}{\pi_\beta(a|s)} - 1 \right]. \quad (\text{F.10})$$

F.4. Conservative Bellman Consistency Equations

Q Functions. Considering the matrix form and point-wise Bellman consistency equation, we have

$$\mathbf{Q}^\pi = \mathbf{r} + \gamma \mathbf{P}^\pi \mathbf{Q}^\pi \implies \mathbf{Q}^\pi = (\mathbf{I} - \gamma \mathbf{P}^\pi)^{-1} \mathbf{r} \quad (\text{F.11})$$

$$\mathbf{Q}^\pi(s, a) = r(s, a) + \gamma [\mathbf{P}^\pi \mathbf{Q}^\pi]_{(s,a)}, \quad \forall (s, a) \in \mathcal{S} \times \mathcal{A}, \quad (\text{F.12})$$

where we use $[\mathbf{P}^\pi \mathbf{Q}^\pi]_{(s,a)}$ to denote the entries $(s, a)^{\text{th}}$ of the matrix $\mathbf{P}^\pi \mathbf{Q}^\pi$. Now recall the point-wise Bellman consistency equation of the CQL objective equation F.1, we also have the following point-wise consistency equation:

$$\mathbf{Q}_{\alpha,\beta}^\pi(s, a) = r(s, a) + \gamma [\mathbf{P}^\pi \mathbf{Q}_{\alpha,\beta}^\pi]_{(s,a)} - \alpha \left[\frac{\pi(a|s)}{\pi_\beta(a|s)} - 1 \right], \quad \forall (s, a) \in \mathcal{S} \times \mathcal{A}, \quad (\text{F.13})$$

$$= r_{\alpha,\beta} + \gamma [\mathbf{P}^\pi \mathbf{Q}^\pi]_{(s,a)}, \quad (\text{F.14})$$

where

$$r_{\alpha,\beta}^\pi(s, a) := r(s, a) - \alpha \left[\frac{\pi(a|s)}{\pi_\beta(a|s)} - 1 \right], \quad \forall (s, a) \in \mathcal{S} \times \mathcal{A}. \quad (\text{F.15})$$

Hence, we can similarly have the bellman-consistency equation of CQL in matrix form:

$$\mathbf{Q}_{\alpha,\beta} = \mathbf{r}_{\alpha,\beta} + \gamma \mathbf{P}^\pi \mathbf{Q}_{\alpha,\beta} \implies \mathbf{Q}_{\alpha,\beta}^\pi = (\mathbf{I} - \gamma \mathbf{P}^\pi)^{-1} \mathbf{r}_{\alpha,\beta}. \quad (\text{F.16})$$

Value Functions. Now considering the Bellman Consistency equation of the Value function, we have

$$\mathbf{V}^\pi = \mathbf{r}^\pi + \gamma \mathbf{P}^\pi \mathbf{V}^\pi \implies \mathbf{V}^\pi = (\mathbf{I} - \gamma \mathbf{P}^\pi)^{-1} \mathbf{r}^\pi \quad (\text{F.17})$$

$$\mathbf{V}_{\alpha,\beta}^\pi = \mathbf{r}_{\alpha,\beta}^\pi + \gamma \mathbf{P}^\pi \mathbf{V}_{\alpha,\beta}^\pi \implies \mathbf{V}_{\alpha,\beta}^\pi = (\mathbf{I} - \gamma \mathbf{P}^\pi)^{-1} \mathbf{r}_{\alpha,\beta}^\pi. \quad (\text{F.18})$$

Summary. In summary, for a given reward function \mathbf{r} , a fixed policy π , a behavior policy π_β , and a fixed constant α , the policy evaluation for CQL satisfies:

$$\begin{aligned} \mathbf{V}_{\alpha,\beta}^\pi &= (\mathbf{I} - \gamma \mathbf{P}^\pi)^{-1} \mathbf{r}_{\alpha,\beta}^\pi = (\mathbf{I} - \gamma \mathbf{P}^\pi)^{-1} \Pi^\pi [\mathbf{r} - \alpha (\pi/\pi_\beta - \mathbf{1})] \\ \mathbf{Q}_{\alpha,\beta}^\pi &= (\mathbf{I} - \gamma \mathbf{P}^\pi)^{-1} \mathbf{r}_{\alpha,\beta} = (\mathbf{I} - \gamma \mathbf{P}^\pi)^{-1} [\mathbf{r} - \alpha (\pi/\pi_\beta - \mathbf{1})]. \end{aligned} \quad (\text{F.19})$$

where $\pi/\pi_\beta \in \mathbb{R}^{|\mathcal{S}| \times |\mathcal{A}|}$ is a vector whose (s, a) entry denotes $\pi(a|s)/\pi_\beta(a|s)$ and $\mathbf{1} = \{1, 1, \dots, 1\}^\top \in \mathbb{R}^{|\mathcal{S}| \times |\mathcal{A}|}$.

F.5. Proof of Theorem F.1

Theorem F.3 (Invariant Conservative Q Functions). *Let $Q_{\alpha,\beta}^\pi$ and $Q_{\alpha',\beta'}^\pi$ denote the conservative value function from solving the conservative bellman consistency equation (Equation F.1 and F.19) with regularizers α, α' and behavior policies $\pi_\beta, \pi_{\beta'}$ respectively. Then for a given policy π , $Q_{\alpha,\beta}^\pi(s) = Q_{\alpha',\beta'}^\pi(s), \forall s \in \mathcal{S}$ if and only if*

$$\frac{\alpha}{\pi_\beta(a|s)} - \frac{\alpha'}{\pi_{\beta'}(a|s)} = \frac{\alpha - \alpha'}{\pi(a|s)}, \quad \forall (s, a) \in \mathcal{S} \times \mathcal{A}. \quad (\text{F.20})$$

Proof. By the conservative Bellman Consistency equation F.19, we know that changing a behavior policy from π_β to $\pi_{\beta'}$ and changing the regularize from α to α' , we have

$$\begin{aligned} Q_{\alpha,\beta}^\pi - Q_{\alpha',\beta'}^\pi &= (\mathbf{I} - \gamma \mathbf{P}^\pi)^{-1} (\mathbf{r}_{\alpha,\beta}^\pi - \mathbf{r}_{\alpha',\beta'}^\pi) \\ &= (\mathbf{I} - \gamma \mathbf{P}^\pi)^{-1} \left[\alpha \left(\frac{\pi}{\pi_\beta} - \mathbf{1} \right) - \alpha' \left(\frac{\pi}{\pi_{\beta'}} - \mathbf{1} \right) \right]. \end{aligned} \quad (\text{F.21})$$

Since $(\mathbf{I} - \gamma \mathbf{P})^{-1}$ is a square and full rank matrix, $Q_{\alpha,\beta}^\pi - Q_{\alpha',\beta'}^\pi = \mathbf{0}$ holds if and only if

$$\alpha \left(\frac{\pi}{\pi_\beta} - \mathbf{1} \right) - \alpha' \left(\frac{\pi}{\pi_{\beta'}} - \mathbf{1} \right) = \mathbf{0} \implies \frac{\alpha}{\pi_\beta(a|s)} - \frac{\alpha'}{\pi_{\beta'}(a|s)} = \frac{\alpha - \alpha'}{\pi(a|s)}, \quad \forall (s, a) \in \mathcal{S} \times \mathcal{A}, \quad (\text{F.22})$$

which finishes the proof. \square

G. Key Results of HyQ (Song et al., 2023)

In this section, we restate the major theoretical results of Hy-Q (Song et al., 2023) for completeness.

G.1. Assumptions

Assumption G.1 (Realizability and Bellman completeness). *For any h , we have $Q_h^* \in \mathcal{F}_h$, and additionally, for any $f_{h+1} \in \mathcal{F}_{h+1}$, we have $\mathcal{T} f_{h+1} \in \mathcal{F}_h$.*

Definition G.2 (Bilinear model Du et al. (2021)). *We say that the MDP together with the function class \mathcal{F} is a bilinear model of rank d if for any $h \in [H - 1]$, there exist two (known) mappings $X_h, W_h : \mathcal{F} \mapsto \mathbb{R}^d$ with $\max_f \|X_h(f)\|_2 \leq B_X$ and $\max_f \|W_h(f)\|_2 \leq B_W$ such that*

$$\forall f, g \in \mathcal{F} : \left| \mathbb{E}_{s,a \sim d_h^\pi} [g_h(s, a) - \mathcal{T} g_{h+1}(s, a)] \right| = |\langle X_h(f), W_h(g) \rangle|. \quad (\text{G.1})$$

Definition G.3 (Bellman error transfer coefficient). *For any policy π , we define the transfer coefficient as*

$$C_\pi := \max \left\{ 0, \max_{f \in \mathcal{F}} \frac{\sum_{h=0}^{H-1} \mathbb{E}_{s,a \sim d_h^\pi} [\mathcal{T} f_{h+1}(s, a) - f_h(s, a)]}{\sqrt{\sum_{h=0}^{H-1} \mathbb{E}_{s,a \sim v_h} (\mathcal{T} f_{h+1}(s, a) - f_h(s, a))^2}} \right\}. \quad (\text{G.2})$$

G.2. Main Theorem of Hy-Q

Theorem G.4 (Theorem 1 of Song et al. (2023)). *Fix $\delta \in (0, 1)$, $m_{\text{off}} = K$, $m_{\text{on}} = 1$, and suppose that the underlying MDP admits Bilinear rank d (Definition G.2), and the function class \mathcal{F} satisfies Assumption G.1. Then with probability at least $1 - \delta$, HyQ obtains the following bound on cumulative suboptimality w.r.t. any comparator policy π^e :*

$$\text{Reg}(K) = \tilde{O} \left(\max\{C_\pi, 1\} V_{\max} B_X B_W \sqrt{d H^2 K \cdot \log(|\mathcal{F}|/\delta)} \right). \quad (\text{G.3})$$

G.3. Key Lemmas

G.3.1. Least Squares Generalization and Applications

Lemma G.5 (Lemma 7 of Song et al. (2023), Online and Offline Bellman Error Bound for FQI). *Let $\delta \in (0, 1)$ and $\forall h \in [H - 1], k \in [K]$, let f_h^{k+1} be the estimated value function for time step h computed via least square regression using samples in the dataset $\{\mathcal{D}_h^v, \mathcal{D}_h^1, \dots, \mathcal{D}_h^T\}$ in equation B.1 in the iteration t of Algorithm 2. Then with probability at least $1 - \delta$, for any $h \in [H - 1]$ and $k \in [K]$, we have*

$$\|f_h^{k+1} - \mathcal{T}f_{h+1}^{k+1}\|_{2, v_h}^2 \leq \frac{1}{m_{\text{off}}} 256 V_{\max}^2 \log(2HK|\mathcal{F}|/\delta) =: \Delta_{\text{off}} \quad (\text{G.4})$$

and

$$\sum_{\tau=1}^k \|f_h^{k+1} - \mathcal{T}f_{h+1}^{k+1}\|_{2, \mu_h^\tau}^2 \leq \frac{1}{m_{\text{on}}} 256 V_{\max}^2 \log(2HK|\mathcal{F}|/\delta) =: \Delta_{\text{on}}, \quad (\text{G.5})$$

where v_h denotes the offline data distribution at time h , and the distribution $\mu_h^\tau \in \Delta(s, a)$ is defined such that $s, a \sim d_h^{\pi^\tau}$.

G.3.2. Bounding Offline Suboptimality via Performance Difference Lemma

Lemma G.6 (Lemma 5 of Song et al. (2023), performance difference lemma of w.r.t. π^e). *Let $\pi^e = (\pi_0^e, \dots, \pi_{H-1}^e)$ be a comparator policy and consider any value function $f = (f_0, \dots, f_{H-1})$, where $f_h : S \times \mathcal{A} \mapsto \mathbb{R}$. Then we have*

$$\mathbb{E}_{s \sim d_0} \left[V_0^{\pi^e}(s) - \max_a f_0(s, a) \right] \leq \sum_{i=1}^{H-1} \mathbb{E}_{s, a \sim d_i^{\pi^e}} [\mathcal{T}f_{i+1}(s, a) - f_i(s, a)], \quad (\text{G.6})$$

where we define $f_H(s, a) = 0, \forall (s, a)$.

G.3.3. Bounding Online Suboptimality via Performance Difference Lemma

Lemma G.7 (Lemma 4 of Song et al. (2023), performance difference lemma). *For any function $f = (f_0, \dots, f_{H-1})$ where $f_h : S \times \mathcal{A} \mapsto \mathbb{R}$ and $h \in [H - 1]$, we have*

$$\mathbb{E}_{s \sim d_0} \left[\max_a f_0(s, a) - V_0^{\pi^f}(s) \right] \leq \sum_{h=0}^{H-1} \left| \mathbb{E}_{s, a \sim d_h^{\pi^f}} [f_h(s, a) - \mathcal{T}f_{h+1}(s, a)] \right|, \quad (\text{G.7})$$

where we define $f_H(s, a) = 0, \forall s, a$.

Lemma G.8 (Lemma 8 of Song et al. (2023), upper bounding bilinear class). *For any $k \geq 2$ and $h \in [H - 1]$, we have*

$$\left| \langle W_h(f^k), X_h(f^k) \rangle \right| \leq \|X_h(f^k)\|_{\Sigma_{k-1, h}^{-1}} \sqrt{\sum_{i=1}^{k-1} \mathbb{E}_{s, a \sim d_h^{\pi^f}} \left[(f_h^k - \mathcal{T}f_{h+1}^k)^2 \right]} + \lambda B_W^2, \quad (\text{G.8})$$

where $\Sigma_{k-1, h}$ is defined as equation B.5 and we use $d_h^{\pi^f}$ to denote $d_h^{\pi^f}$.

Lemma G.9 (Lemma 6 of Song et al. (2023), bounding the inverse covariance norm). *Let $X_h(f^1), \dots, X_h(f^K) \in \mathbb{R}^d$ be a sequence of vectors with $\|X_h(f^k)\|_2 \leq B_X < \infty, \forall k \leq K$. Then we have*

$$\sum_{k=1}^K \|X_h(f^k)\|_{\Sigma_{k-1, h}^{-1}} \leq \sqrt{2dK \log \left(1 + \frac{KB_X^2}{\lambda d} \right)}, \quad (\text{G.9})$$

where we define $\Sigma_{k; h} := \sum_{\tau=1}^k X_h(f^\tau) X_h(f^\tau)^T + \lambda \mathbf{I}$ and we assume $\lambda \geq B_X^2$ holds $\forall k \in [K]$.